remote sensing

MDPI

Article

Leaf Spectra Changes of Plants Grown in Soils Pre- and Post-Contaminated with Petroleum Hydrocarbons

Salete Gürtler [1,2,*], Carlos R. Souza Filho [1], Ieda D. Sanches [3], Lucíola A. Magalhães [2], Marcos N. Alves [4], Wilson J. Oliveira [1] and Giuliana C. M. Quitério [1]

[1] Institute of Geosciences, University of Campinas (UNICAMP), P.O. Box 6152, Campinas 13083-970, SP, Brazil; beto@unicamp.br (C.R.S.F.); wilsonjo@petrobras.com.br (W.J.O.); giuliana.clarice@vemprafam.com.br (G.C.M.Q.)
[2] Territorial Intelligence Unit, Brazilian Agricultural Research Corporation (EMBRAPA), Av. Soldado Passarinho, 303, Fazenda Jardim Chapadão, Campinas 13070-115, SP, Brazil; luciola.magalhaes@embrapa.br
[3] Earth Observation and Geoinformatics Division, National Institute for Space Research (INPE), P.O. Box 515, São José dos Campos 12227-010, SP, Brazil; ieda.sanches@inpe.br
[4] Pluridisciplinary Center for Chemical, Biological and Agricultural Research (CPQBA), University of Campinas (UNICAMP), P.O. Box 6171, Campinas 13081-970, SP, Brazil; mnopper@cpqba.unicamp.br
* Correspondence: salete.gurtler@colaborador.embrapa.br

Abstract: Leaks from accidents or damage to pipelines that transport liquid petroleum hydrocarbons (PHC) such as gasoline and diesel are harmful to the environment as well as to human health, and may be hard to detect by inspection mechanisms alone when they occur in small volumes or persistently. In the present study, we aim to identify spectral anomalies in two plant species (*Brachiaria brizantha* and *Neonotonia wightii*) linked to contamination effects at different developmental phases of these plants. To do so, we used spectroscopy and remote sensing approaches to detect small gasoline and diesel leaks by observing the damage caused to the vegetation that covers simulated pipelines. We performed a contamination test before and after planting using gasoline and diesel volumes that varied between 2 and 16 L/m^3 soil, in two experimental designs: (i) single contamination before planting, and (ii) periodic contaminations after planting and during plant growth. We collected the reflectance spectra from 35 to approximately 100 days after planting. We then compared the absorption features positioned from the visible spectral range to the shortwave infrared and the spectral parameters in the red edge range of the contaminated plants to the healthy plants, thus confirming the visual and biochemical changes verified in the contaminated plants. Despite the complexity in the indirect identification of soil contamination by PHCs, since it involves different stages of plant development, the results were promising and can be used as a reference for methods of indirect detection from UAVs (Unmanned Aerial Vehicles), airplanes, and satellites equipped with hyperspectral sensors.

Keywords: reflectance spectroscopy; contamination; liquid hydrocarbons; vegetation stress; hyperspectral

Citation: Gürtler, S.; Souza Filho, C.R.; Sanches, I.D.; Magalhães, L.A.; Alves, M.N.; Oliveira, W.J.; Quitério, G.C.M. Leaf Spectra Changes of Plants Grown in Soils Pre- and Post-Contaminated with Petroleum Hydrocarbons. *Remote Sens.* **2022**, *14*, 3475. https://doi.org/10.3390/rs14143475

Academic Editors: Sophie Fabre, Arnaud Elger and Guillaume Lassalle

Received: 10 June 2022
Accepted: 14 July 2022
Published: 20 July 2022

1. Introduction

The Brazilian pipeline network covers 20,000 km, transporting natural gas, petroleum, and petroleum products. It interconnects producing regions, platforms, marine terminals, refineries, and distribution bases [1].

Most of the pipelines are underground and protected by an approximately 1-m thick superficial soil layer. They are susceptible to weather, terrain movement, changes in temperature, and human action, which may damage them, resulting in leakages that are hard to detect. Petroleum hydrocarbons (PHCs) are highly flammable and contaminant to the environment. Conventional monitoring methods, often performed by field operators, have limited reach to identify small leaks [2,3]. Techniques that enable regular pipeline monitoring that can rapidly identify and locate isolated leaks are scarce.

Since soil and vegetation occupy most of the superficial layer that covers the pipelines, we assume that persistent soil contamination with liquid PHCs in small amounts affects the upper-layer plant cover, which may indicate the location and extent of the problem. In the specific case of diesel (DSL), the movement of DSL in soil layers is low, even after vegetation onset and constant irrigation, due to its low water solubility [4]. In contact with roots, PHCs hamper plant growth and development, causing reductions to root and shoot masses, and sometimes even the complete extinction of early-stage vegetation [4–6]. PHC compounds fill the spaces in the soil preventing water and air movement, which causes soil compaction and leads to the degradation of its biological, physical, and chemical properties [6].

Considering the same species, changes in morphology and biochemical content triggered by senescence processes or stress can ultimately modify the spectral response of the plants [7,8]. Spectral changes caused by PHC contamination in vegetation have been assessed in situ by reflectance spectroscopy and imaging spectroscopy in several studies [5,9–19].

Vegetation spectral properties are the result of vegetation bio-parameters. Plants show sensitivity to these properties at different spectral ranges, such as visible (VIS), near infrared (NIR) and shortwave infrared (SWIR) [20]. Specific regions of the spectrum may show changes in the contents of chlorophylls and carotenoids (around 420, 490 and 660 nm), water content (around 900, 1200, 1400 and 1900 nm) and biochemical compounds (around 1750 and 2300 nm) [8,21–24]. The red edge region (between 690 and 720 nm) is particularly sensitive to vegetation stress and to changes in total chlorophyll content, rendering it one of the most investigated regions [8,24].

Recently published literature reviews have highlighted the need to study the different effects of stress on different species considering a longer timescale than those based on single-date measurements [20], focusing on identifying the most relevant plant species, and, for each, the types of petroleum products and concentration ranges that can be identified or quantified [2].

There have been very few studies using reflectance spectroscopy to evaluate PHC effects on plant development from the germination phase in contaminated soils, particularly the effects of liquid PHCs. Ref. [5] analyzed the effect of natural gas contamination and concluded that it affected crops of wheat and bean during their seeding phases. In contrast, when they released gas to full-grown plant canopies, they observed no effects, probably because the root system had already been formed and was able to obtain water and nutrients outside the gas influence zone. The authors explain that the presence of PHCs in the soil inhibits respiration and nutrient and water absorption by the roots, affecting plants more strongly in their early developmental phase than when their canopies are already developed. The result is plant atrophy, with plants showing smaller leaves and root systems. However, little is known about the spectral changes that occur in plants germinated in soils contaminated with liquid PHCs.

In this context, our objective here is to identify spectral anomalies (in the visible and infrared regions of the electromagnetic spectrum) in two plant species (*Brachiaria brizantha* and *Neonotonia wightii*), grown in pre- (before planting) and post- (after planting and plant growth) contaminated soils with different volumes of gasoline and diesel, under semi-controlled environmental conditions.

2. Material and Methods

2.1. Plant Species Studied

Brachiaria (*Brachiaria brizantha* H.S.; Poaceae) is a commonly found crop along petroleum pipelines in Brazil. Easily adaptable to different climate conditions, it is not very demanding in terms of soil fertility. It has a varied root system and reaches a depth of 1 m.

Perennial soybean (*Neonotonia wightii* Arn.; Fabaceae), a climbing plant that grows well in high-altitude regions, is a legume of African origin widely used in combined pastures.

Despite its initial slow growth, the plant shows quick evolution and has a deep root system. It produces green biomass of excellent quality after its establishment.

2.2. Field Experiment

Two experiments (soil contaminated before planting (SCBefore) and soil contaminated after planting (SCAfter)) were set up under semi-controlled conditions in a greenhouse equipped with shading screens on its sides, plastic rooftop and an automatic irrigation system (Figure 1) in an experimental field at The University of Campinas (Campinas, Brazil).

Figure 1. Experiment installed inside the greenhouse.

The experiments used slightly different set-ups regarding lysimeter material, scheme of contamination and number of species (Figure 2).

2.2.1. Experiment with Soil Contamination before Planting (SCBefore)

For SCBefore, 100 lysimeters (with 40, 30 and 20-cm height, width and depth, respectively), which can host 24 L of material each, were built using black, high-density polyethylene containers. To build the lysimeters, the upper part of the containers was removed and silicon hoses were installed for contaminant distribution. These hoses were installed parallel to the soil, forming a central line along the planting line, at a 15-cm depth. To guarantee homogeneous contaminant application to the soil, the hoses were perforated to produce equally spaced holes throughout.

The lysimeters were filled with homogenized soil (Rhodic Ferralsol with 65% of clay) and placed along four benches inside the greenhouse, with equal spacing between one another and the irrigation nozzle (Figure 3A).

SCBefore was performed using brachiaria (BR) (SCBefore-BR) and perennial soybean (PS) (SCBefore-PS) as stress indicators. Contaminants were applied in two different, separate ways. Firstly, we used injection pumps made of plastic (SCBefore-BR, Figure 3B). The contaminant was spilled in a central pit, which was then covered with soil. The soil layer kept the PHCs at approximately 15 cm from the surface. Secondly, we produced a surficial homogeneous spill on the planting line (SCBefore-PS, Figure 3C). Changes in the form of contaminant application between the BR and PS steps aimed to simplify the method, ensuring soil contamination homogeneity.

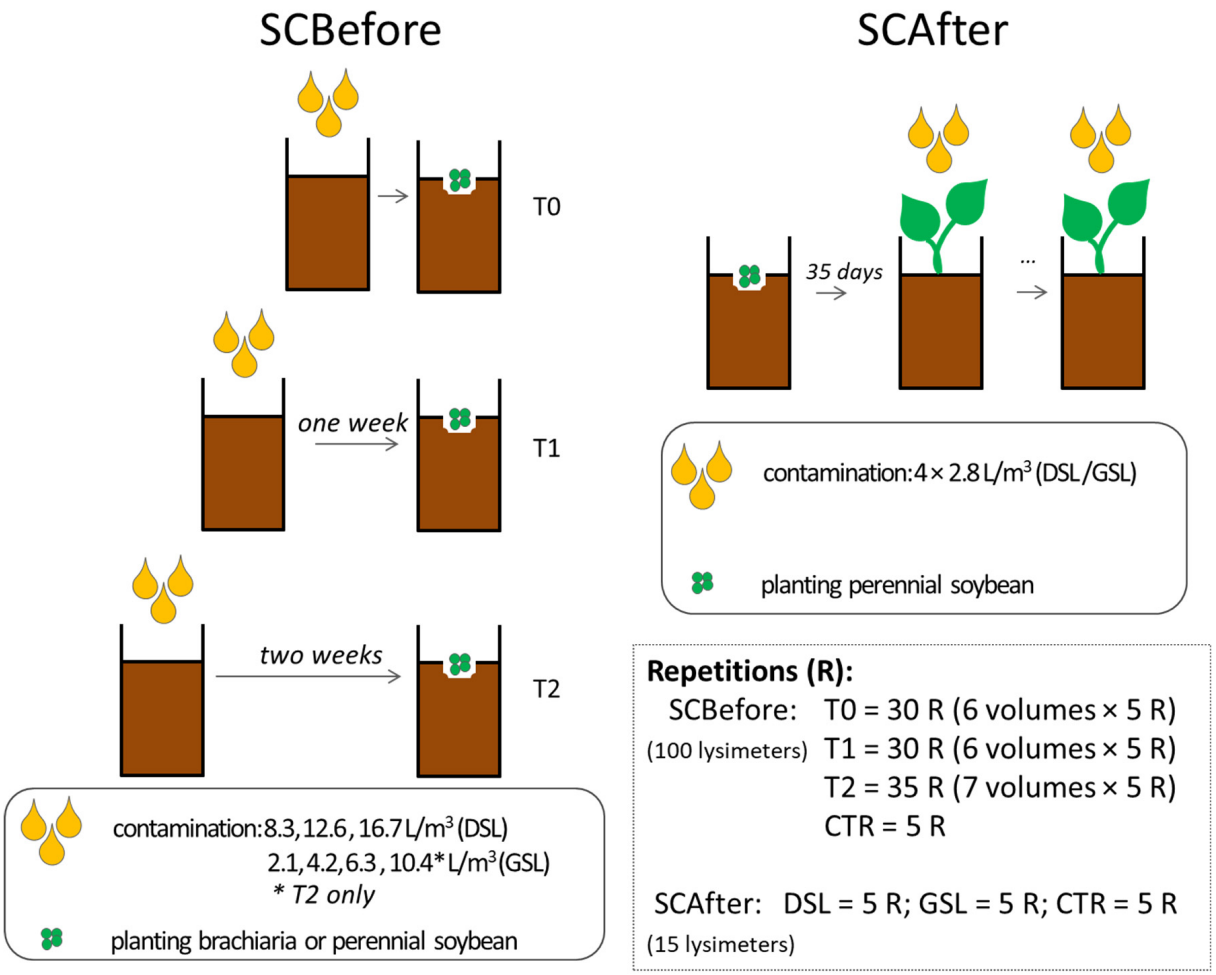

Figure 2. Sampling design scheme with five repetitions for each treatment.

(**A**) (**B**) (**C**)

Figure 3. Photos of the SCBefore installation: (**A**) Lysimeters on the benches and internal view of the greenhouse; (**B**) PHC application using an injection pump for the brachiaria (BR) experiment (SCBefore-BR), simulating an underground leakage. (**C**) PHC application simulating a surficial spill for the perennial soybean (PS) experiment (SCBefore-PS).

2.2.2. Experiment with Soil Contamination after Planting (SCAfter)

For SCAfter, we used 15 glass lysimeters, measuring 30 cm in length, 40 cm in height, and 15 cm in width. We inserted a hose with equally spaced holes into the lysimeter at a 20-cm depth from the surface, allowing a homogeneous application of the contaminants in the soil after plant growth.

2.3. Treatments

The contaminants used were common gasoline (GSL) and diesel (DSL), both commercial fuels. They were acquired in small quantities (1–5 L) at a local petrol station. In Brazil, common GSL contains 25% ethanol for reducing carbon monoxide emissions in automobile engines. The DSL used was common B S500 biodiesel (diesel with a 0.05% sulphur addition).

2.3.1. SCBefore Treatment

In the experiment, we used different contaminant volumes defined according to dosage and field experiments previously carried out [13,14] (Table 1). We then applied DSL in concentrations between 8.3 and 16.7 L/m^3. GSL concentrations were smaller and ranged between 2.1 and 10.4 L/m^3, as previous experiments [13,14] op. Cit showed a more aggressive initial effect of GSL than that of DSL, which might have killed the plants' embryos, making the seeds unviable.

Table 1. Volumes and exposure time of contaminants in the SCBefore. GSL: gasoline. DSL: diesel.

Contaminant	Volume per Lysimeter (mL)	L/m^3	Exposure Time
GSL	50	2.1	T0, T1, T2
	100	4.2	T0, T1, T2
	150	6.3	T0, T1, T2
	250	10.4	T2
DSL	200	8.3	T0, T1, T2
	300	12.6	T0, T1, T2
	400	16.7	T0, T1, T2

T0 = no exposure before planting; T1 = contaminated one week before planting; and T2 = contaminated two weeks before planting.

Before sowing, we applied different exposure times to soil contaminants: T0 (no exposure before planting); T1 (contaminated one week before planting); and T2 (contaminated two weeks before planting). We used all exposure times (T0, T1 and T2) for all contaminant concentrations, except 10.4 L/m^3 (GSL), for which we only tested T2. The exposure time may reduce the volatile fraction in PHCs, which is responsible for reducing germination by killing the embryo [25,26]. The absence of exposure or a shorter exposure time at a higher concentration can be extremely aggressive for the embryo, making sprouting impossible and the experiment impractical.

Lysimeters distribution inside the greenhouse followed a completely randomized design (total of 100 lysimeters, with five replicates for each treatment. We considered three volumes for GSL and DSL, with three exposure times each, and one volume for GSL, with only one exposure, in addition to the control (CTR).

We planted seeds scarified with concentrated sulfuric acid, to breach embryo dormancy (10 BR seeds and 15 PS seeds laid on a straight line at the central part of each lysimeter). To guarantee a synchronized growth of the plants under treatment, we began the experiment two weeks before planting the seeds, at which time we contaminated the T2 lysimeters, differently from the T1 lysimeters, which we contaminated one week later.

2.3.2. SCAfter Treatment

We randomly placed all 15 lysimeters (3 treatments: GSL, DSL and CTR, 5 replicates) on the benches inside the greenhouse. Thirty-five days after planting, PS plants were well established, and the first contaminant dose was applied. Doses of 50 mL of PHC (GSL and DSL) were applied in each lysimeter through the distribution hoses buried at 20 cm from the soil surface. We carried out four application rounds at 14-day intervals to reach an accumulated volume of 200 mL in each lysimeter.

2.4. Collection of Spectral Data

We performed the spectral measurements in situ using an ASD FieldSpec® 4 spectroradiometer to which we coupled a plant probe and a leaf clip (accessories by ASD Inc., Westborough, MA, USA, [27,28]). This spectroradiometer comprises three sensors that cover the spectral range 350–2500 nm, with 2151 channels, and spectral resolutions of 3 nm @ 700 nm and 8 nm @ 1400/2100 nm. Its sampling interval is 1.4 nm @ 350–1050 nm and 2 nm @ 1000–2500 nm. For the reflectance measurements, we used a Spectralon® (Labsphere, North Sutton, NH, USA) plate as a reference.

We applied two data collection methods to each experiment:

i. We measured SCBefore, 10 BR leaves and 5 PS leaves (adaxial side) from each lysimeter, to obtain a representative average spectrum for each replicate. The smaller number of PS leaves sampled (5 instead of 10 leaves) was due to the insufficient number of leaves developed in the more aggressive treatments. In some cases, PS failed to develop many leaves or the size of the leaves was too small to be sampled and analyzed. Each leaf measurement is equivalent to the average of 25 readings. Along the experiment, four spectral measurements were performed for each experiment, at approximately every two weeks (55, 67, 84 and 95 days after planting-DAP-for BR, and 50, 63, 77 and 91 DAP for PS) (Table 2). Each complete measurement lasted from 2 to 3 days. We took BR measurements between September and November 2012, and PS measurements between February and March 2013. Although the crops were grown at different times, we respected all the planting recommendations of the seed producer. In addition, semi-controlled conditions ensured uniform water supply and aerial cover ensured protection from seasonal pests.
ii. We measured SCAfter, using two PS leaves (adaxial side) from each lysimeter. We performed seven measurements starting at 35 DAP, when the plants were well established; the last one being at 99 DAP (Table 2).

Table 2. Spectral measurements and accumulated volume of contaminant in each experiment. DAP = days after planting. GSL: gasoline. DSL: diesel.

SCBefore-BR			SCBefore-PS			SCAfter-PS	
DAP	**GSL (L/m^3)**	**DSL (L/m^3)**	**DAP**	**GSL (L/m^3)**	**DSL (L/m^3)**	**DAP**	**GSL and DSL (L/m^3)**
55	2.1, 4.2, 6.3, 10.4	8.3, 12.6, 16.7	50	2.1, 4.2, 6.3, 10.4	8.3, 12.6, 16.7	35	0
67	2.1, 4.2, 6.3, 10.4	8.3, 12.6, 16.7	63	2.1, 4.2, 6.3, 10.4	8.3, 12.6, 16.7	49	2.8
84	2.1, 4.2, 6.3, 10.4	8.3, 12.6, 16.7	77	2.1, 4.2, 6.3, 10.4	8.3, 12.6, 16.7	56, 64	5.6
95	2.1, 4.2, 6.3, 10.4	8.3, 12.6, 16.7	91	2.1, 4.2, 6.3, 10.4	8.3, 12.6, 16.7	79, 84	8.3
						99	11.1

2.5. Processing and Analysis of Spectral Data

We first calculated the mean absolute reflectance spectra for each lysimeter, and drew characteristic curves for each treatment. The PRISM (Processing Routines in IDL for Spectroscopic Measurements; [29]) program was used to process spectral data. Data on the plant spectral response were analyzed based on the visible (VIS: between 400 and 700 nm), near infrared (NIR: between 700 and 1000 nm) and shortwave infrared (SWIR: between 1000 and 2500 nm) portions of the electromagnetic spectrum. We selected eight absorption features for analysis with continuum removal (two in VIS, two in NIR, and four in SWIR). We evaluated them to allow the possibility of differentiating plants developed in contaminated soil from healthy plants (Figure 4).

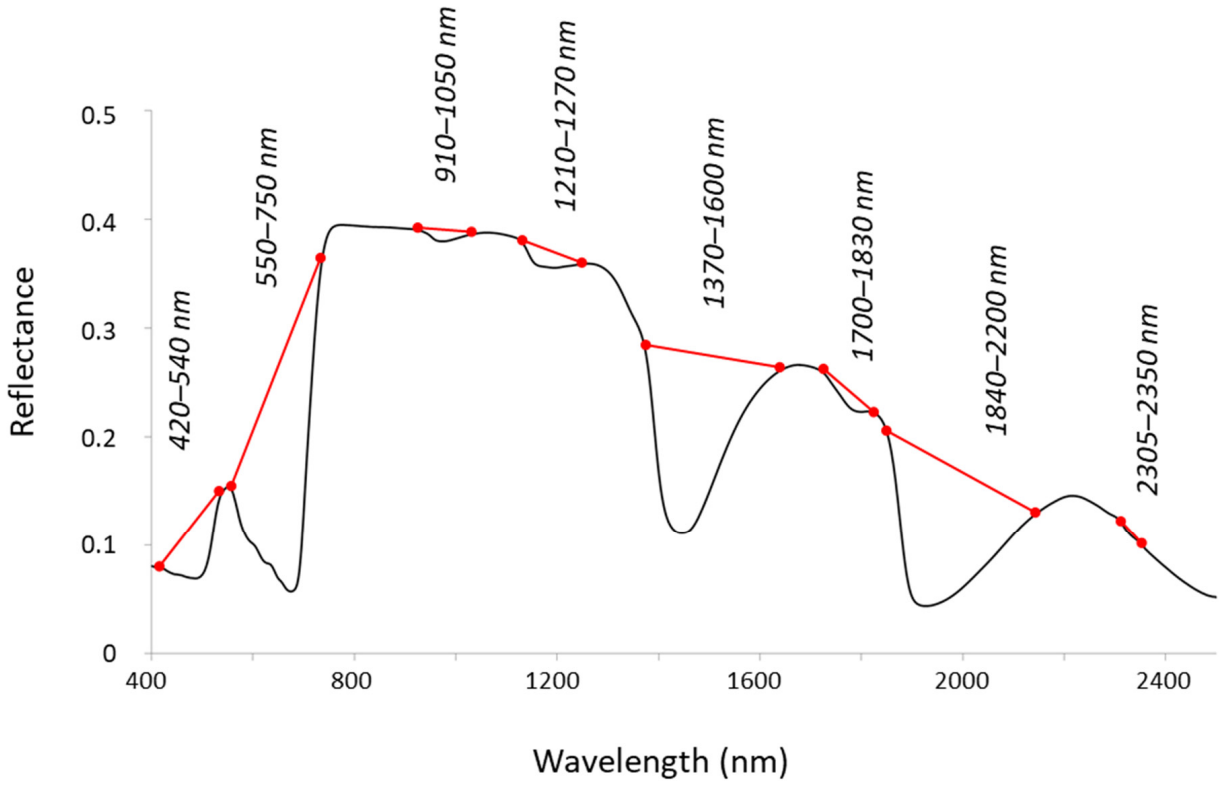

Figure 4. Absorption features analyzed using the continuum removal method; continuum line shown in red.

We used the continuum removal method to compare absorption features: the reflectance spectra are normalized and the feature of interest is enhanced [30] The spectral intervals used here correspond to ranges where the vegetation absorption features are prominent, which are widely documented in the literature [21–24]. In this study, continuum removal was applied to two pigment absorption features (420–540 and 550–750 nm), four water absorption features (910–1050; 1210–1270; 1370–1600; 1840–2200 nm) and two organic compound absorption features (1725–1825 and 2305–2350 nm).

We investigated the red edge region in greater detail due to its importance for the study of stressed plants [31] and used the red edge position method and first-derivative reflectance ratio at 725 and 702 nm (FD725/FD702) [5] in the analyses.

Vegetation reflectance in the visible range is dominated by the absorption capacity of photosynthetic pigments. The 660 and 680 nm features are attributed to chlorophylls a and b. Studies show that red edge shift to shorter wavelengths (blue shift) is directly related to a decrease in chlorophyll concentration [32–34].

This shift may be assessed by means of the red edge position (REP), which is the wavelength at which the maximum score of the reflectance spectra first derivative between 680 and 760 nm occurs. The first derivative of the average reflectance spectra for the leaves was calculated using The Unscrambler (version 10.3; [35]) software and the Savitzky–Golay method (second-degree polynomial and three smoothing points). The first derivative was used to calculate not only the REP, but also the ratio between the first derivative for the 725 and 702 nm wavelengths (FD725/FD702).

Ref. [5] used a band ratio based on the occurrence of a maximum score in the first derivative spectra, between 720 and 730 nm, and a lower score around 702 nm. Below 700 nm, there is a predominance of the absorption attributed to chlorophyll. Absorption decreases at 725 nm, and energy is scattered in direct proportion to pigment concentration [32].

2.6. Biochemical (Plant) and Total Petroleum Hydrocarbon (Soil) Analysis

After the last spectral measurement (95 DAP for SCBefore-BR, 91 DAP for SCBefore-PS, and 99 DAP for SCAfter-PS), the aerial parts of the plants (leaves and stems) were entirely collected and prepared for fresh and dry mass weighing. We separated a small portion of fresh leaves and sent them to the laboratory for biochemical analysis (chlorophyll a and b and carotenoids). The vegetation water content (VWC) was calculated as follows [36]. Fresh weight (FW) and dry weight (DW) refer to the same sample.

$$\text{VWC} = (\text{FW} - \text{DW})/\text{FW} \times 100\ (\%)$$

For the SCBefore, soil samples with the highest volumes of contaminants (GSL = 6.3 and DSL = 16.7 L/m^3, at T0, T1 and T2) were collected out of 3 lysimeters for each treatment, for total petroleum hydrocarbon (TPH) analysis. The samples were collected after the soil surface layer was removed in order to reach the contaminated region.

3. Results and Discussion

3.1. Visual Effects of Contaminants in Plant Development

The plants grown in soils contaminated with GSL and DSL were visually different from healthy plants (CTR) in both experiments (SCBefore and SCAfter). Contamination with PHCs affected the development of the studied species, reducing their aerial biomass as well as their root formation.

Under SCBefore, the aerial parts of both BR and PS plants did not show homogeneous development during different treatments. There was a direct correlation between plant development and PHC volumes in the soil. The most affected plants were those treated with the highest PHC volumes.

BR-CTR plants were vigorous in the first spectral measurement at 55 DAP (Figure 5), while plants under the BR-DSL and BR-GSL treatments showed fewer plants with smaller leaves. In some cases (21 lysimeters, 18 contaminated with DSL and 3 contaminated with GSL), it was not possible to perform all 10 measurements foreseen for each lysimeter due to an absence of big enough leaves to use a leaf clip (at 55 DAP). The DSL can reach the upper plant parts (stems and leaves) when transported from the roots along the plant transpiration stream [37]. In *Scirpus grossus*, DSL caused changes to the leaves (yellowing and size reduction), stems, and roots. Scanning electron microscopy revealed irregular and reduced internal forms, thus confirming DSL adsorption to the plants' surface instead of accumulation in their internal tissue [38]. After 67 DAP, the plants showed signs of relative recovery, and exhibited similar leaf growth during the treatments.

Germination of PS seeds was affected mainly in the lysimeters containing GSL, which showed a reduced number of plants, and even an absence of plants in four lysimeters. DSL had a less severe effect on germination, and only one lysimeter showed no plants, a situation that changed along the vegetation development. DSL affected plants more severely, causing considerable reduction in leaf size, as observed in some concentrations until the end of the experiment (91 DAP) (Figure 6).

In SCAfter, the plants grown in GSL and DSL contaminated soil were visually distinct from the healthy plants (CTR). Contamination by the two PHCs significantly affected the development of PS, reducing roots and aboveground fresh shoots. Visually, DSL and especially GSL plants showed some leaves with chlorosis (Figure 7). The magnitude of the toxic effect (decreased germination, survival and development of leaves, stems and roots) is determined by the biological characteristics of each plant species and the type and concentration of the contaminant [39,40].

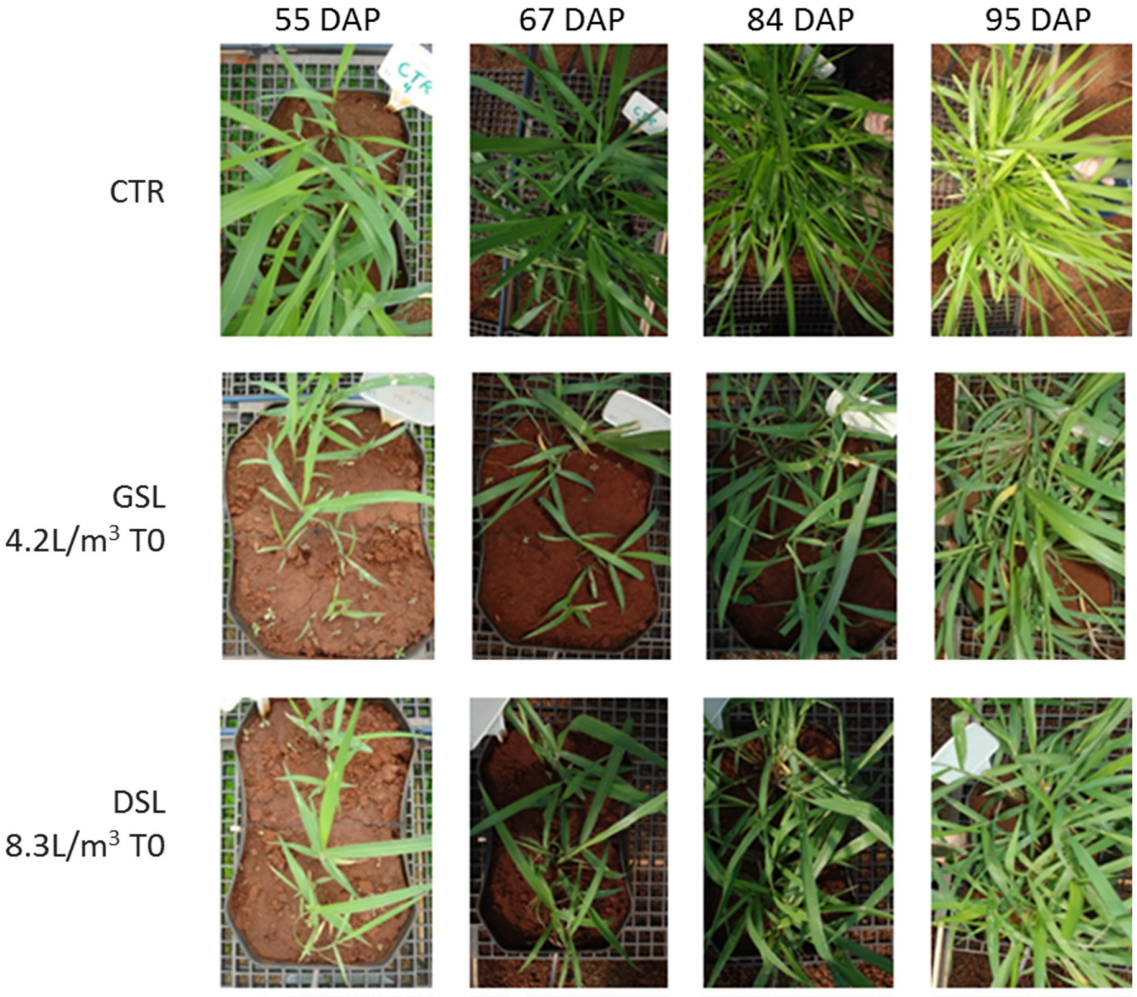

Figure 5. Top view of the lysimeters for SCBefore-BR under CTR, GSL (4.2 L/m^3, T0: no exposure) and DSL (8.3 L/m^3, T0) treatments at 55, 67, 84 and 95 DAP (DAP = days after planting).

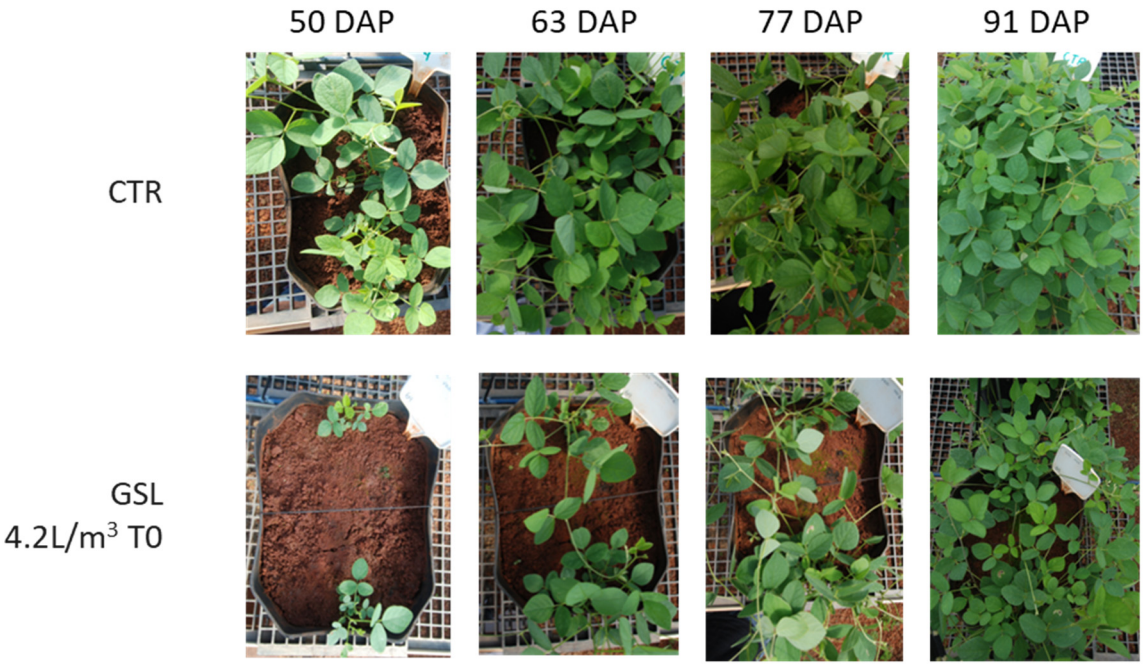

Figure 6. *Cont.*

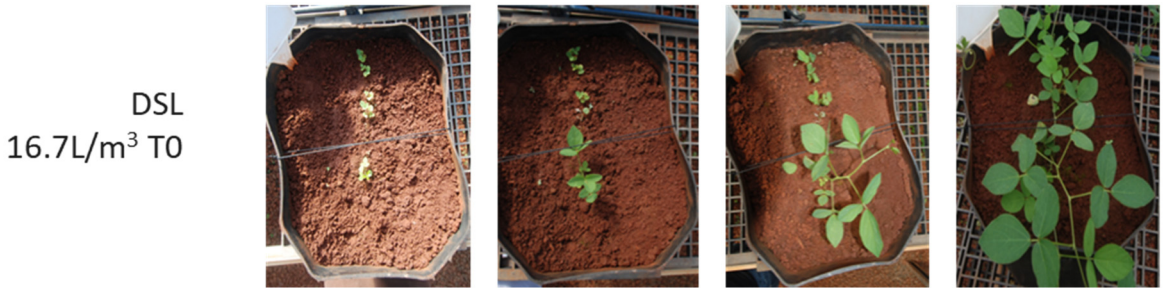

Figure 6. Top view of the lysimeters for SCBefore-PS under CTR, GSL (4.2 L/m^3, T0: no exposure) and DSL (16.7 L/m^3, T0) treatments at 50, 63, 77 and 91 DAP (DAP = days after planting).

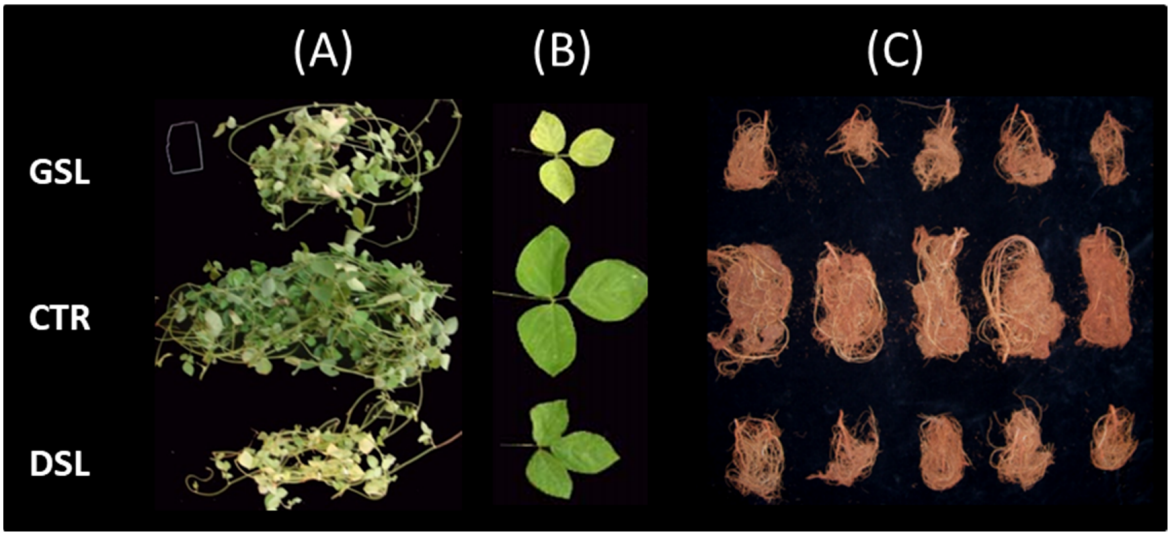

Figure 7. Comparative photographs of fresh plants SCAfter-PS grown in soil contaminated with DSL, GSL and not contaminated (CTR) at 99 DAP: (**A**) shoot, (**B**) leaves and (**C**) roots.

3.2. Morpho-Physiological Analyses

The mean fresh weight (MFW) at the end of the experiment showed the impact in aerial biomass production caused by contamination (Figure 8). Under SCBefore, there was a correlation of MFW decrease with contaminant concentration increase and with exposure time decrease. MFW reduction in SCBefore was more relevant for DSL than for GSL, due to the larger volumes applied. Under SCAfter, in which the volumes applied were identical, GSL (18% of MFW-CTR) affected MFW more than DSL (23% of MFW-CTR).

Considering the SCBefore-PS grown in soil contaminated with GSL and with exposure time (T1-2.1, T1-4.2 L/m^3 and T2-all concentrations), leaf and stem production was more expressive (up to 228 g) than that of healthy plants (157 g). The longer the exposure time, the stronger the PHC volatile fraction reduction, which may justify its lower impact on plant production. Ref. [25] observed that DSL inhibited germination, but that 50 days after contamination the effects were inverse, i.e., plants grown in contaminated soil were favored when compared to those grown in the control treatment. The authors suggest that volatile compounds disappear from the soil over time, and other compounds found in diesel are not toxic to the seed and microorganisms in the soil. Besides, the carbon now available becomes a new source of energy and nutrients for both the plant and the microorganisms [25,41]. Ref. [42] compared a legume species with a grass species and observed that the former was less affected by PHCs, which, according to them, is due to the association between legumes and nitrogen-fixing microorganisms.

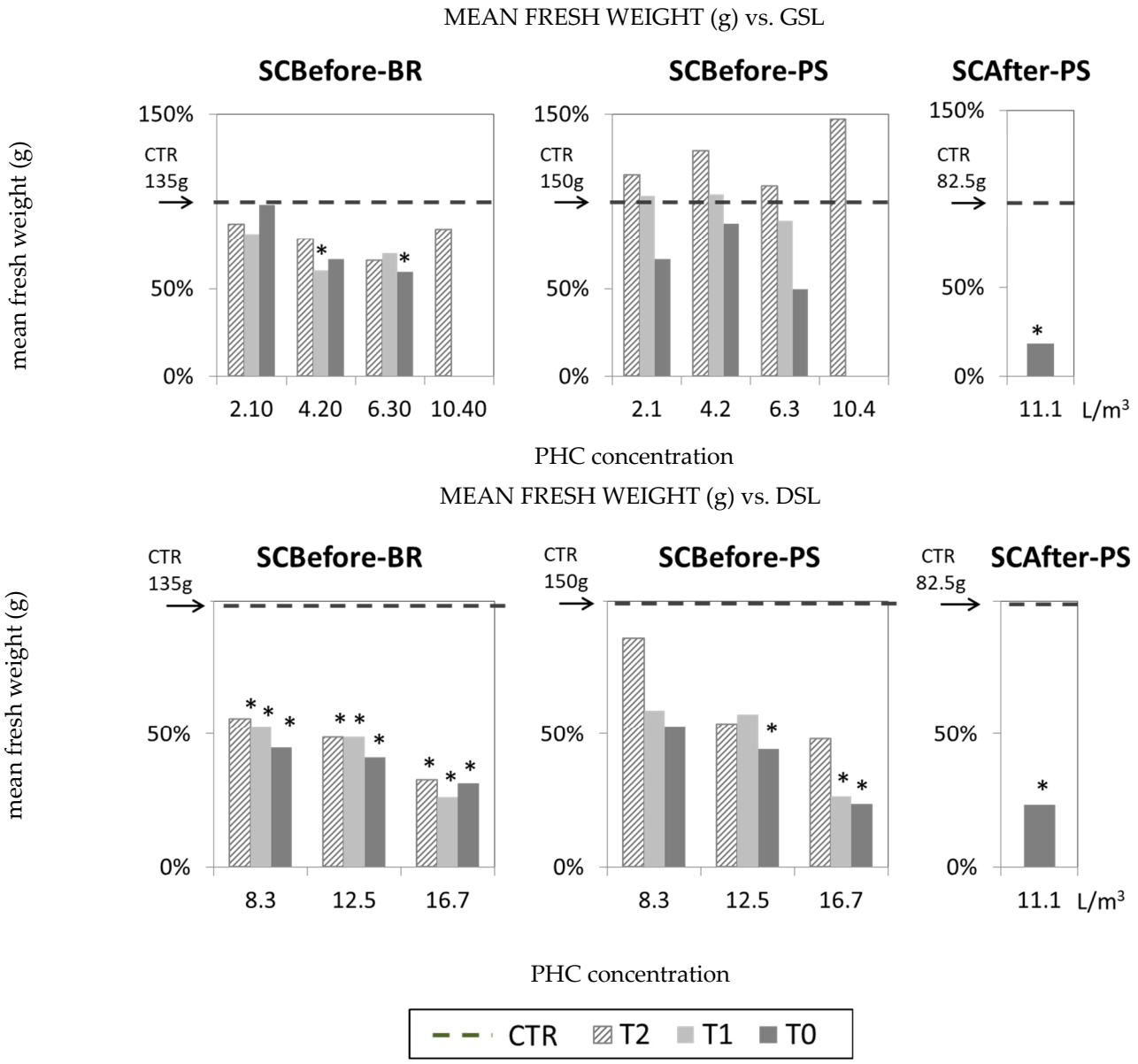

Figure 8. Fresh weight of the aerial part of BR (SCBefore) and PS (SCBefore and SCAfter) contaminated with GSL and DSL when compared with CTR. DAP = Days after planting. * Different averages compared with the averages for the control treatment, according to the *t*-test ($p \leq 0.05$).

PHCs had an inverse effect on the plants when it comes to water content (Figure 9), considering the analyzed plant development phase (90 DAP). Except for SCAfter-DSL, the affected plants, under all the remaining treatments, showed increased water content in leaves and stems when compared to that of healthy plants. The larger the contaminant volume, the larger the water concentration observed in the plants. A possible explanation is that plants exposed to water scarcity regulate water loss through transpiration by closing their stomata [43]. We also observed increasing reductions in maize transpiration rates with an increase in DSL dose [16]. Although the experimental conditions were controlled (all treatments were provided with the same volumes of water), the contaminants may have formed a physical barrier that repels water, which impairs water absorption and gas exchange by the roots. Other authors [25,26,40] detected that diesel has a hydrophobic effect in the soil, thus hindering plant germination and growth.

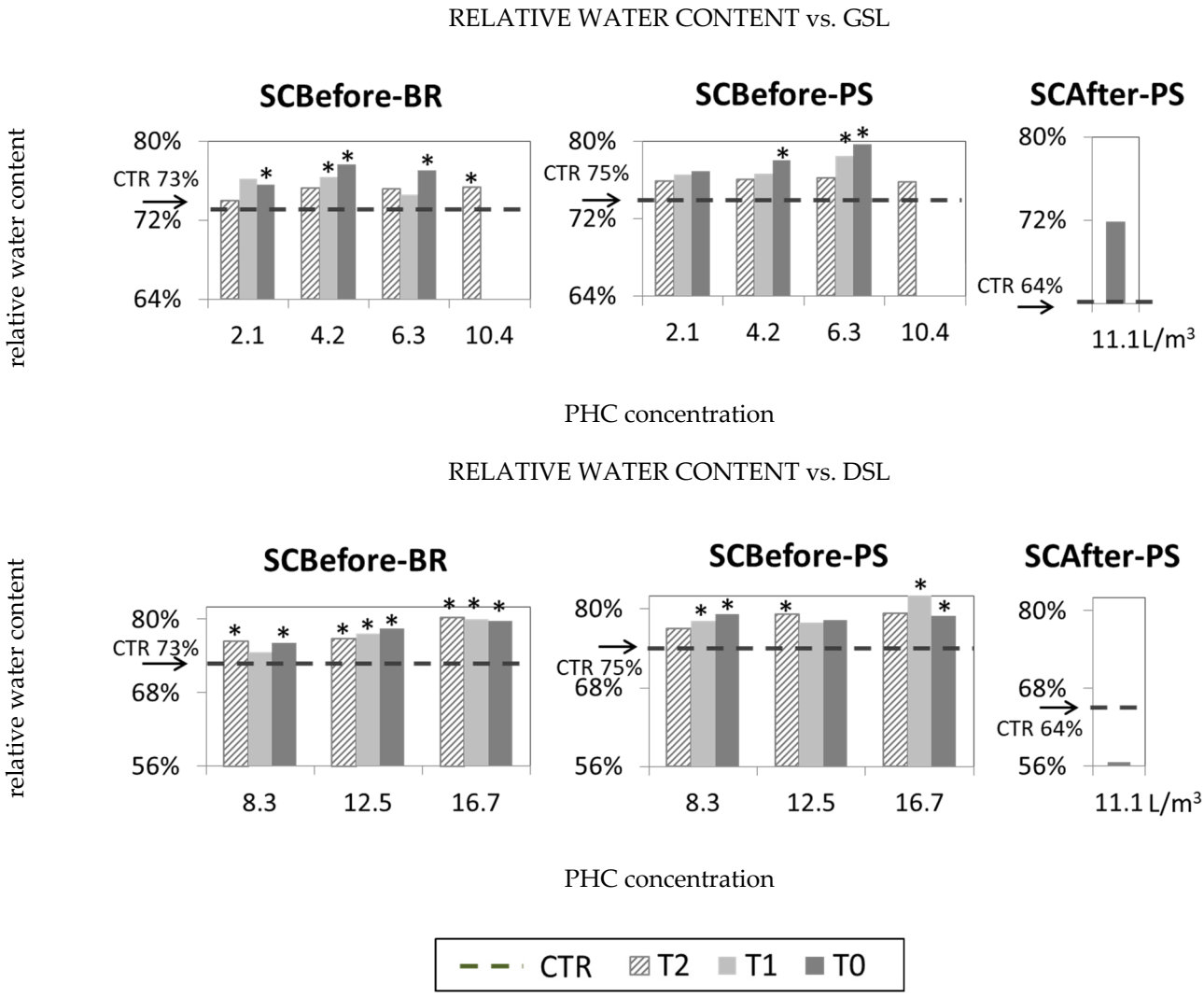

Figure 9. Vegetation water content in the aerial part of BR (SCBefore) and PS (SCBefore and SCAfter) contaminated with GSL and DSL when compared with CTR. DAP = Days after planting. * Different averages compared with the averages for the control treatment, according to *t*-test ($p \leq 0.05$).

3.3. Biochemical and Soil Analysis

Three months after soil contamination, the average of chlorophyll and carotenoid contents for BR grown in contaminated soil was substantially higher than that detected in CTR plants (Figures 10 and 11). Considering that the exposure time may attenuate the damaging effects on plants, since part of the volatile fraction may be reduced, the most aggressive contaminant levels (highest concentrations in T0) show higher contents of these pigments. For BR, at this developmental phase, the contaminant in the soil favored chlorophyll concentration, perhaps to compensate for the reduction in leaf area, thus increasing energy production performance.

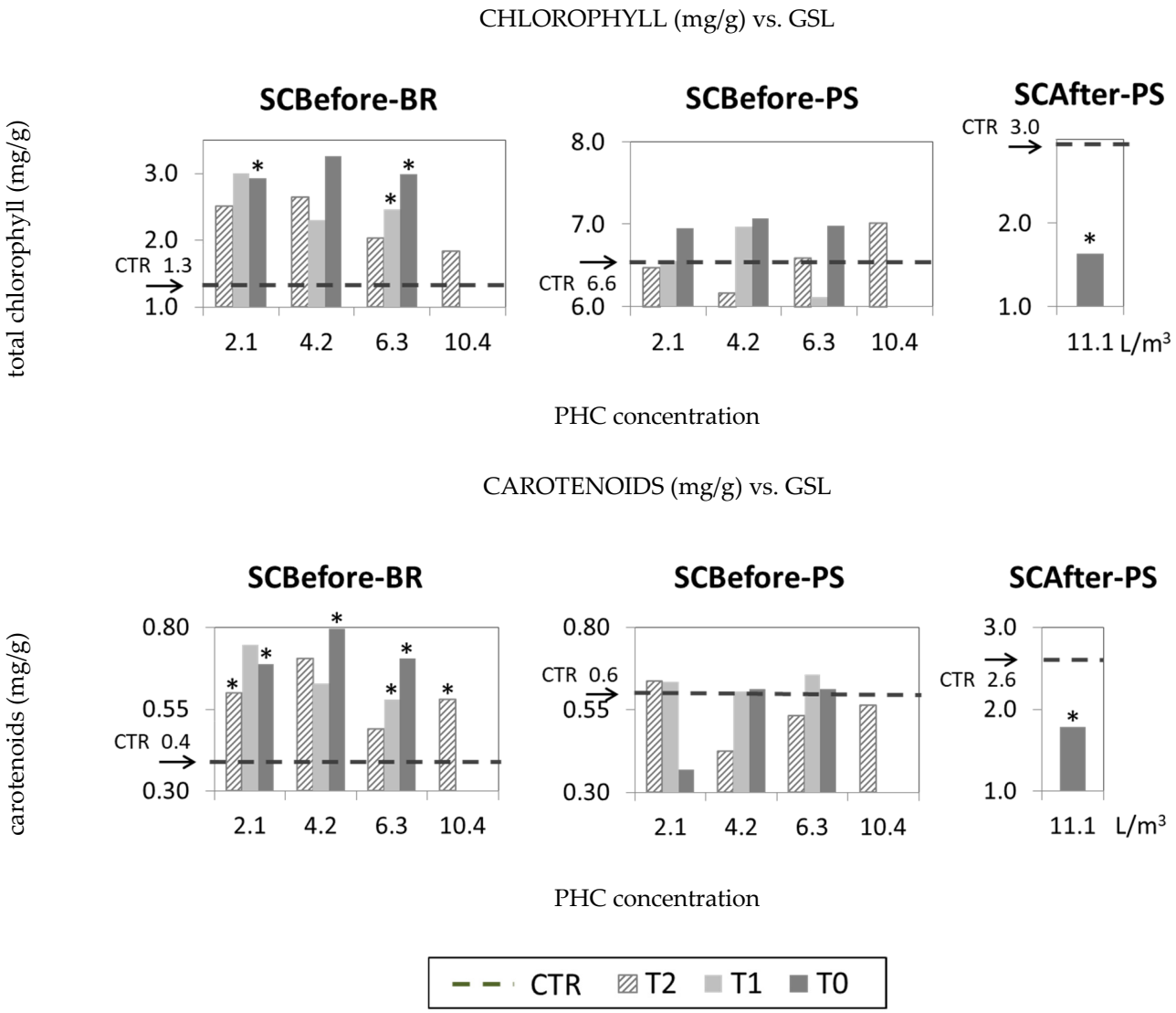

Figure 10. CHLOROPHYLL and CAROTENOIDS for BR (SCBefore) and PS (SCBefore and SCAfter) with GSL compared to CTR. DAP = Days after planting. * Different averages compared with the averages for the control treatment, according to *t*-test ($p \leq 0.05$).

We observed the opposite in relation to PS (Figure 11). For SCBefore-PS, we detected no significant differences in terms of pigment contents, whereas for SCAfter-PS, the same pigments displayed significantly lower levels.

Studies show there is no consensus regarding changes to these contents in plants contaminated with PHCs. Ref. [44] did not identify important differences in pigment content in plants (*Trifolium repens* and *Lolium perenne*) contaminated with DSL (12 g diesel/kg soil) in comparison to healthy plants, even though their roots and sprouts were severely reduced.

Other studies show a reduction in pigment contents caused by PHC contamination. Ref. [45] obtained lower chlorophyll indexes in grasses contaminated with gas. Ref. [14] detected lower concentrations of chlorophyll (in brachiaria, perennial soybean, and maize) and carotenoids (in brachiaria) during DSL and GSL applications. At the end of the contamination, which amounted to 12.7 L/m^3, only chlorophyll-a in perennial soybean contaminated with DSL showed contents lower than those of uncontaminated plants. According to the authors, this was due to plant recovery after the suppression of the stressing agent.

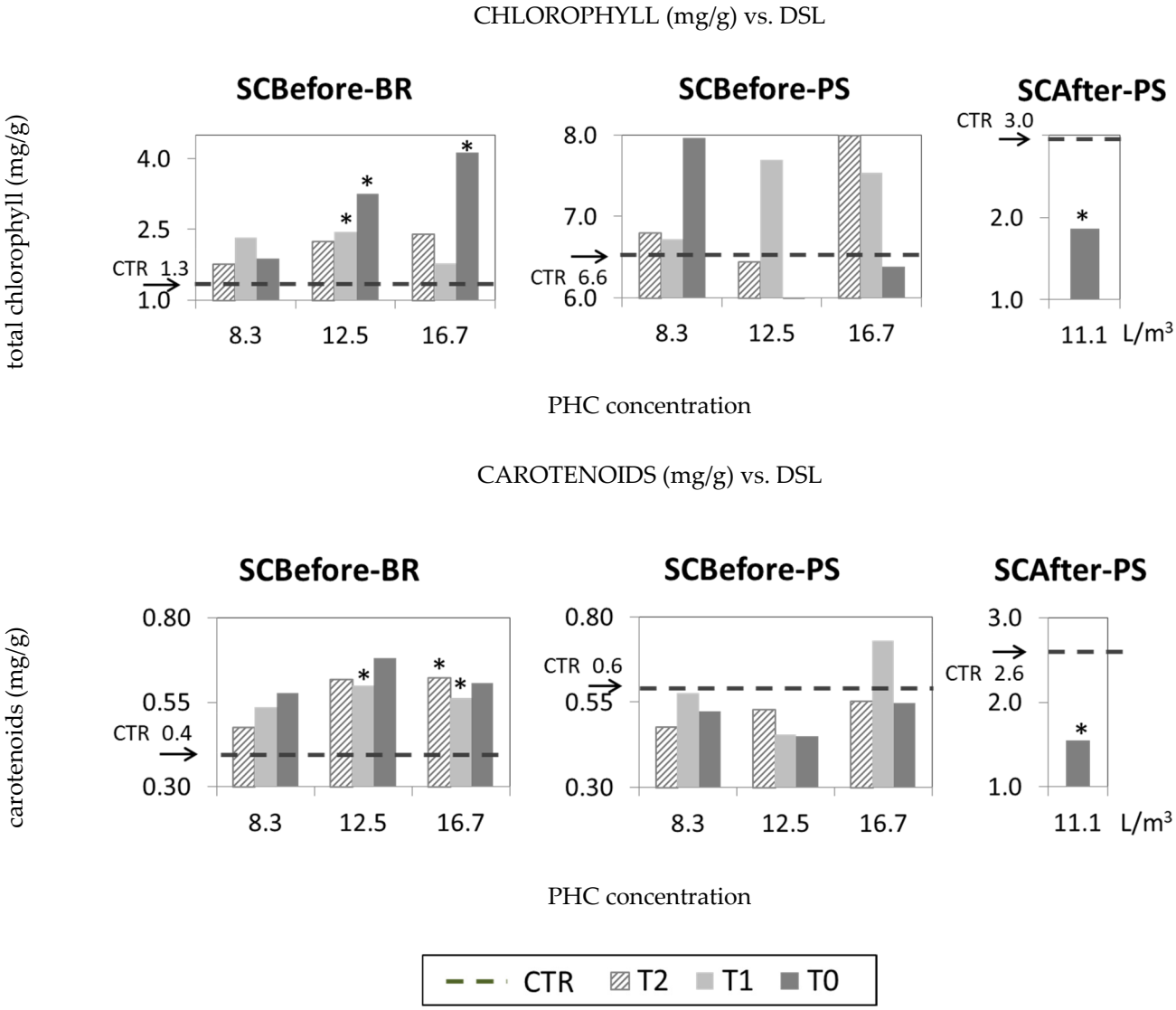

Figure 11. CHLOROPHYLL and CAROTENOIDS for BR (SCBefore) and PS (SCBefore and SCAfter) with DSL compared to CTR. DAP = Days after planting. * Different averages compared with the averages for the control treatment, according to *t*-test ($p \leq 0.05$).

Ref. [46] identified a positive effect of low doses (up to 1%) of DSL on a *Juncus* species 50 days after treatment, with a significant increase in chlorophyll contents following an increase in contaminant concentration. However, chlorophyll contents were considerably lower under higher contaminant concentrations.

3.4. Vegetation Spectral Response

By analyzing the average spectrum for the SCBefore-BR and PS (SCBefore and SCAfter), we identified the effects of soil contamination by PHCs on the leaf spectra at different contamination moments (before and after planting).

The largest contaminant volumes (6.3 L/m^3 for GSL and 16.7 L/m^3 for DSL) caused a reduction in reflectance under SCBefore-BR at 55 DAP when compared to that of healthy plants: average reduction of approximately 10% in VIS and NIR (11% and 8% in VIS-GSL and NIR-GSL; 9% and 12% in VIS-DSL and NIR-DSL) (Figure 12, SCBefore). In the NIR, reflectance remained reduced in comparison to that of CTR up until 95 DAP for both contaminants (reduction in 11 and 18% for GSL and DSL, respectively). Considering the different PHC concentrations applied to SCBefore (GSL: 2.1; 4.2; 6.3; 10.4 L/m^3 and DSL:

8.3; 12.5; 16.7 L/m^3), the average reflectance for BR generally decreased (which increased CTR difference) under both GSL and DSL treatments.

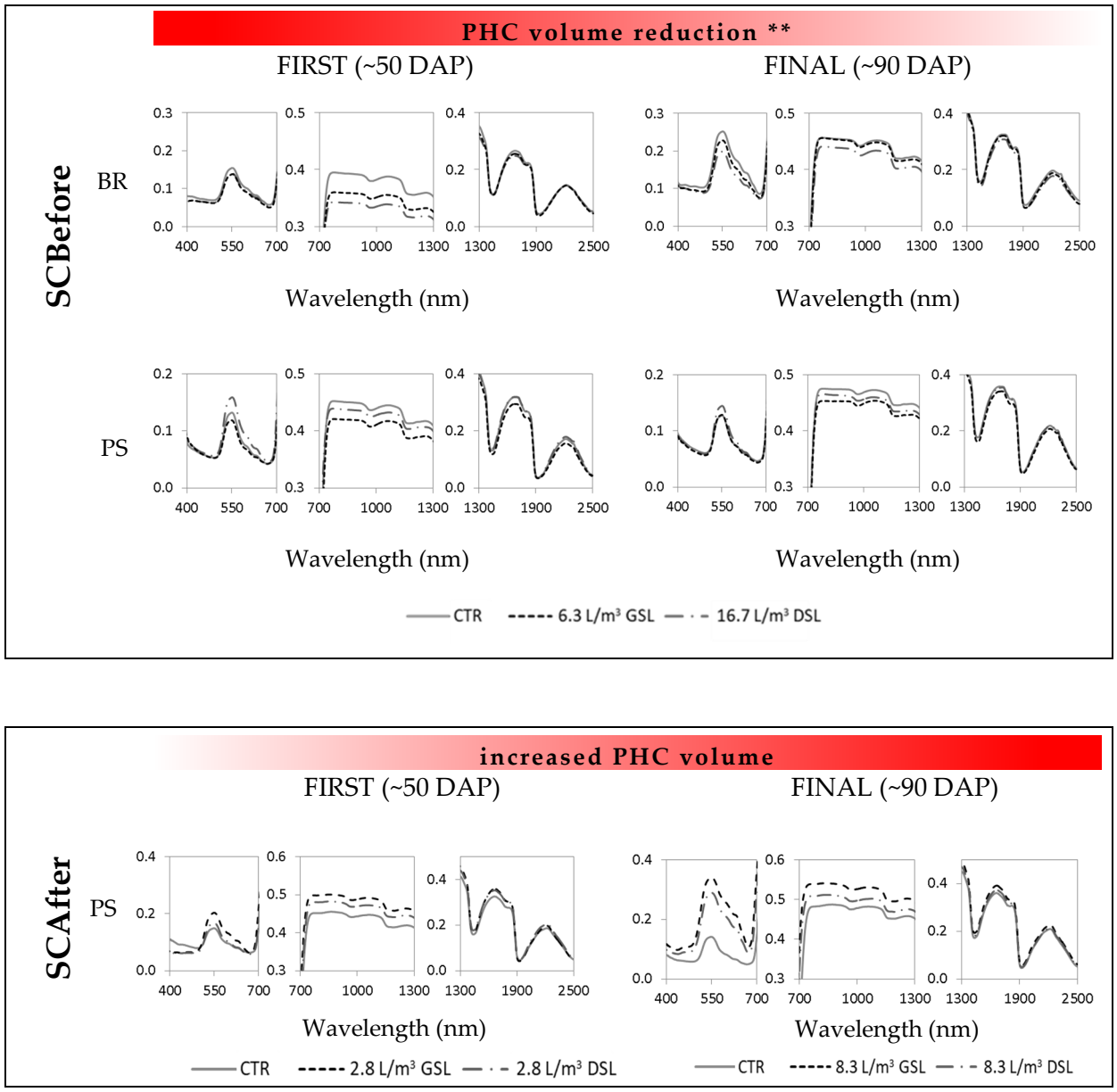

Figure 12. Average leaf reflectance for BR and PS (SCBefore and SCAfter) at approximately 50 and 90 days after planting (DAP). ** Considering a reduction in PHC volume over time, due to the volatilization.

Reflectance for contaminated SCBefore-PS also showed less expressive reductions between 400 and 2500 nm. Plants contaminated with DSL showed stronger reflectance in VIS when compared to that of uncontaminated plants (from 55 DAP to 95 DAP) and are an exception. On a real scale, we observed the same spectral behavior for the PS planted in soil contaminated with DSL [47].

When applied after plant development (SCAfter-PS), PHCs caused an increase in reflectance when compared to that of CTR (Figure 12, SCAfter), which is consistent with similar studies on the contamination of grown plants [13,48]. Under higher concentrations, this increase was even more significant, especially in the VIS range. This range has been considered particularly sensitive to soil contamination because at an early stage (13–25 days) it

shows a higher reflectance rate for contaminated plants when compared to that of control plants until the end of the experiment (61 days) [48].

The contamination timing (before or after planting) greatly affected plant development, and consequently its spectral reflectance. Planting in pre-contaminated soil impaired the plant, causing delayed and reduced development and preventing the leaves from reaching a reflectance level compatible with that of healthy vegetation. Reflectance variations in the NIR range are controlled mainly by leaf anatomical structure [7,24,49]. Thus, the changes observed in the spectra may indicate that the contaminants affected the plant morphology.

The highest chlorophyll and carotenoid concentrations detected in the biochemical analyses for SCBefore-BR (DSL and GSL) contributed to greater absorption around 450 and 650 nm. For the same features, absorption levels similar to (SCBefore-PS) or less deep than (SCAfter-PS) the PS-CTR feature is also in agreement with concentrations equivalent to or smaller than those of photosynthetic pigments in contaminated plants.

Absorption Features after Continuum Removal

We assessed absorption features according to their depth. Their variations may indicate a larger or smaller amount of certain elements that compose the leaves: chlorophyll, carotenoids, leaf water and other organic compounds, such as starch, lignin, cellulose, protein and sugars. In this study, we observed natural variations, which are similar among healthy (control-CTR) plants of both species (*Brachiaria* and *perennial soybean*) along their development (Figures 13–15): (i) the features related to absorption attributed to leaf pigments (420–540 nm and 550–750 nm) had little variation between the first and last measurements; (ii) there was a reduction in depth of the features related to water content inside the leaves: 910–1050 nm; 1210–1270 nm; 1370–1600 nm; 1840–2200 nm; (iii) in the SWIR range, where the absorption features of organic compounds are found (1725–1825 nm and 2305–2350 nm), we observed an increase in feature depth, except for PS1 at 1725–1825 nm, which indicates that these elements accumulate during the plant development.

Comparatively, the same features behaved similarly in healthy plants and under SCBefore (Figures 13 and 14). We observed small decreases in feature depth (related mainly to water in the leaves and non-photosynthetic biochemical compounds) in the first measurement (~50 DAP). This behavior practically disappeared in the last measurement (~90 DAP). The absorption features at 420–520 nm and 550–750 nm, which are related to photosynthetic pigments, maintained lower-depth absorption rates under SCBefore-PS and SCBefore-BR, even 90 days after contamination. There was also a steady lower absorption for the 1840–2140-nm feature of the BR spectrum. According to Jensen (2000), leaf-water absorption features in the SWIR range are more sensitive to water stress. The presence of absorption features with lower depths in the NIR region occurs only in cases of severe leaf dehydration.

SCAfter-PS absorption features related to photosynthetic pigments underwent opposite changes after contaminant application (Figure 15). For the feature between 550 and 750 nm there was a lower absorption in leaves contaminated with up to 11.1 L/m^3 (~100 DAP), whereas in the 440–540 nm range there was an increase in depth and feature area for concentrations up to 8.3 L/m^3 of GSL and DSL. For higher volumes of these contaminants, the feature was similar to that of CTR.

Sanches et al. (2013) [13] also observed a reduction in feature depth for pigments (550–750 nm), as well as in features related to water (1380–1550 and 1850–2000 nm) and to biochemical compounds (2006–2196 nm), in leaf spectra of brachiaria contaminated with PHCs.

PHC volume reduction **

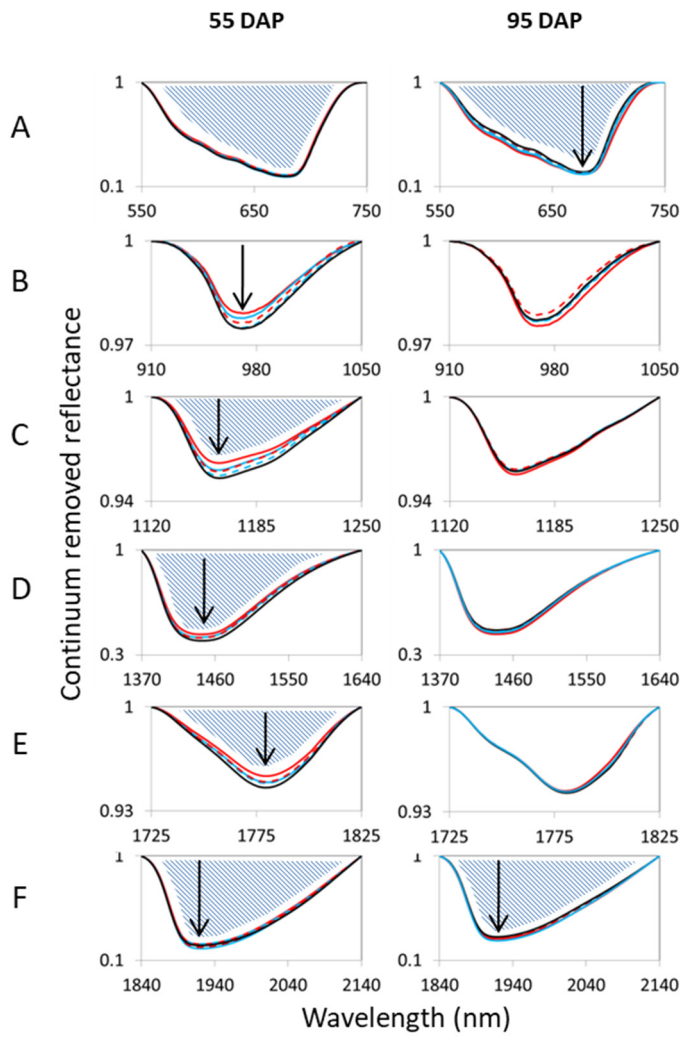

	55 DAP		95 DAP	
	AREA	DEPTH	AREA	DEPTH
CTR	95.76	0.188	81.36	0.225
2.1 L/m² (T2) GSL	94.00	0.201	84.90	0.217
6.3 L/m² (T0) GSL	96.12	0.182	**87.54***	**0.205***
8.3 L/m² (T2) DSL	95.74	0.187	83.25	0.218
16.7 L/m² (T0) DSL	**92.59***	0.198	90.84	**0.209***
CTR	1.64	0.975	1.39	0.977
2.1 L/m² (T2) GSL	1.61	0.975	1.45	0.977
6.3 L/m² (T0) GSL	1.39	0.978	1.42	0.977
8.3 L/m² (T2) DSL	1.50	0.976	1.27	0.979
16.7 L/m² (T0) DSL	1.34	**0.979***	1.55	0.975
CTR	3.37	0.953	2.96	0.957
2.1 L/m² (T2) GSL	3.23	0.955	3.02	0.956
6.3 L/m² (T0) GSL	2.99	0.958	2.99	0.956
8.3 L/m² (T2) DSL	3.01	0.957	2.89	0.958
16.7 L/m² (T0) DSL	**2.74***	**0.962***	3.07	0.955
CTR	87.82	0.395	76.53	0.465
2.1 L/m² (T2) GSL	84.07	**0.415***	78.15	0.456
6.3 L/m² (T0) GSL	82.78	0.417	78.60	0.449
8.3 L/m² (T2) DSL	83.45	0.414	76.28	0.466
16.7 L/m² (T0) DSL	**79.72***	**0.437***	81.08	0.437
CTR	2.89	0.946	3.18	0.943
2.1 L/m² (T2) GSL	2.73	0.949	3.14	0.943
6.3 L/m² (T0) GSL	2.72	0.949	3.12	0.943
8.3 L/m² (T2) DSL	2.69	0.950	3.15	0.943
16.7 L/m² (T0) DSL	**2.45***	**0.954***	3.06	0.944
CTR	141.59	0.229	121.90	0.303
2.1 L/m² (T2) GSL	137.39	0.242	123.57	0.301
6.3 L/m² (T0) GSL	143.20	**0.203***	**128.90***	**0.269***
8.3 L/m² (T2) DSL	140.99	0.214	123.82	0.293
16.7 L/m² (T0) DSL	**135.93***	0.242	128.25	0.284

CTR — 8.3 L/m²(T2) DSL — 16.7 L/m²(T0) DSL — 2.1 L/m²(T2) GSL — 6.3 L/m²(T0) GSL

DSL or GSL spectra area are significantly different from CTR spectra are (*t*-test, $p \leq 0.05$)

DSL or GSL spectra depth are significantly different from CTR spectra are (*t*-test, $p \leq 0.05$)

value* DSL or GSL spectra area or depth are significantly different from CTR spectra are (*t*-test, $p \leq 0.05$)

Figure 13. Leaf reflectance (SCBefore-BR) after continuum removal for the absorption features: (**A**) 550–750 nm; (**B**) 910–1050 nm; (**C**) 1120–1250 nm; (**D**) 1370–1640 nm; (**E**) 1725–1825 nm and (**F**) 1840–2140 nm. ** Considering a reduction in PHC volume over time due to volatilization.

PHC volume reduction **

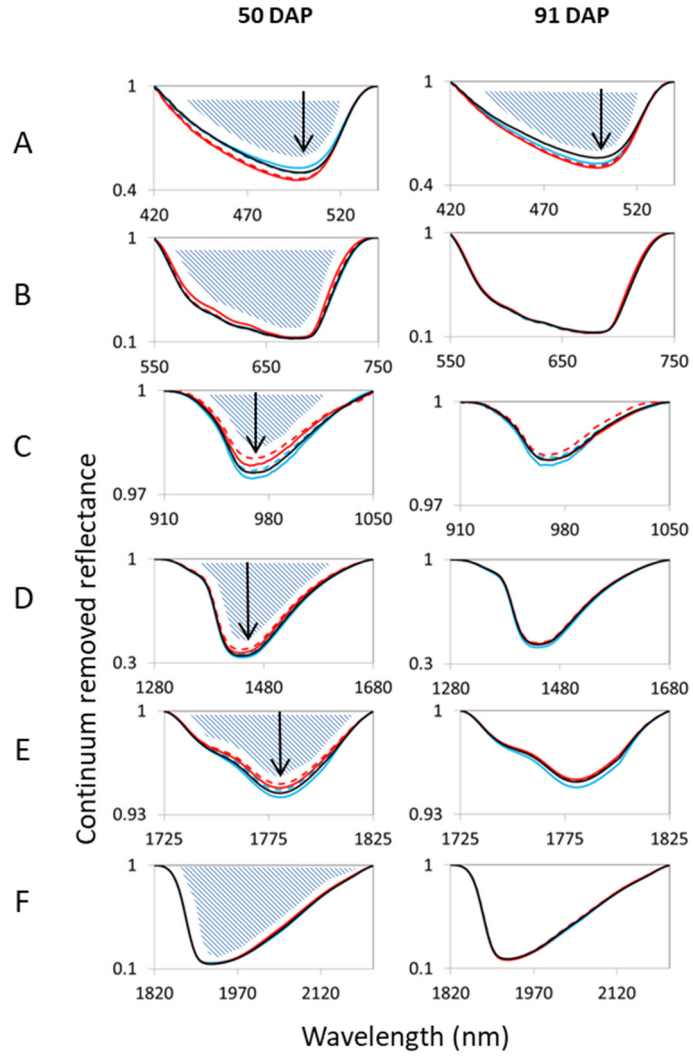

	50 DAP		91 DAP	
	AREA	DEPTH	AREA	DEPTH
CTR	35.81	0.502	31.74	0.600
2.1 L/m² (T2) GSL	36.35	0.532	**35.50***	0.525
6.3 L/m² (T0) GSL	34.49	0.488	34.11	**0.511***
8.3 L/m² (T2) DSL	**38.86***	0.468	35.25	0.513
16.7 L/m² (T0) DSL	**39.71***	**0.459***	35.93	**0.501***
CTR	111.49	0.131	112.07	0.138
2.1 L/m² (T2) GSL	112.19	0.143	112.08	0.135
6.3 L/m² (T0) GSL	111.38	0.128	111.43	0.129
8.3 L/m² (T2) DSL	109.64	0.129	110.71	0.133
16.7 L/m² (T0) DSL	**103.94***	0.139	109.87	0.132
CTR	1.54	0.976	1.01	0.983
2.1 L/m² (T2) GSL	1.50	0.975	0.99	0.982
6.3 L/m² (T0) GSL	1.64	0.978	1.11	0.984
8.3 L/m² (T2) DSL	**1.26***	**0.980***	0.88	0.984
16.7 L/m² (T0) DSL	1.37	0.978	1.05	0.983
CTR	106.91	0.349	90.97	0.430
2.1 L/m² (T2) GSL	105.49	0.335	89.65	0.411
6.3 L/m² (T0) GSL	110.39	0.369	95.00	0.436
8.3 L/m² (T2) DSL	**97.65***	**0.391***	88.83	0.441
16.7 L/m² (T0) DSL	102.10	0.368	89.83	0.435
CTR	3.036	0.945	2.624	0.952
2.1 L/m² (T2) GSL	2.939	0.942	2.565	0.948
6.3 L/m² (T0) GSL	3.196	0.948	2.829	0.953
8.3 L/m² (T2) DSL	**2.691***	**0.951***	2.577	0.953
16.7 L/m² (T0) DSL	2.816	0.948	2.519	0.954
CTR	177.589	0.142	160.829	0.183
2.1 L/m² (T2) GSL	176.501	0.154	160.311	0.177
6.3 L/m² (T0) GSL	178.781	0.141	163.503	0.179
8.3 L/m² (T2) DSL	**170.380***	0.146	158.687	0.182
16.7 L/m² (T0) DSL	173.557	0.145	161.020	0.174

CTR — 8.3 L/m²(T2) DSL — 16.7 L/m²(T0) DSL — 2.1 L/m²(T2) GSL — 6.3 L/m²(T0) GSL

DSL or GSL spectra area are significantly different from CTR spectra are (*t*-test, $p \leq 0.05$)

DSL or GSL spectra depth are significantly different from CTR spectra are (*t*-test, $p \leq 0.05$)

value* DSL or GSL spectra area or depth are significantly different from CTR spectra are (*t*-test, $p \leq 0.05$)

Figure 14. Leaf reflectance (SCBefore-PS) after continuum removal for the absorption features: (**A**) 450–540 nm; (**B**) 550–750 nm; (**C**) 910–1050 nm; (**D**) 1280–1680 nm; (**E**) 1725–1825 nm and (**F**) 1820–2215 nm. ** Considering a reduction in PHC volume over time due to volatilization.

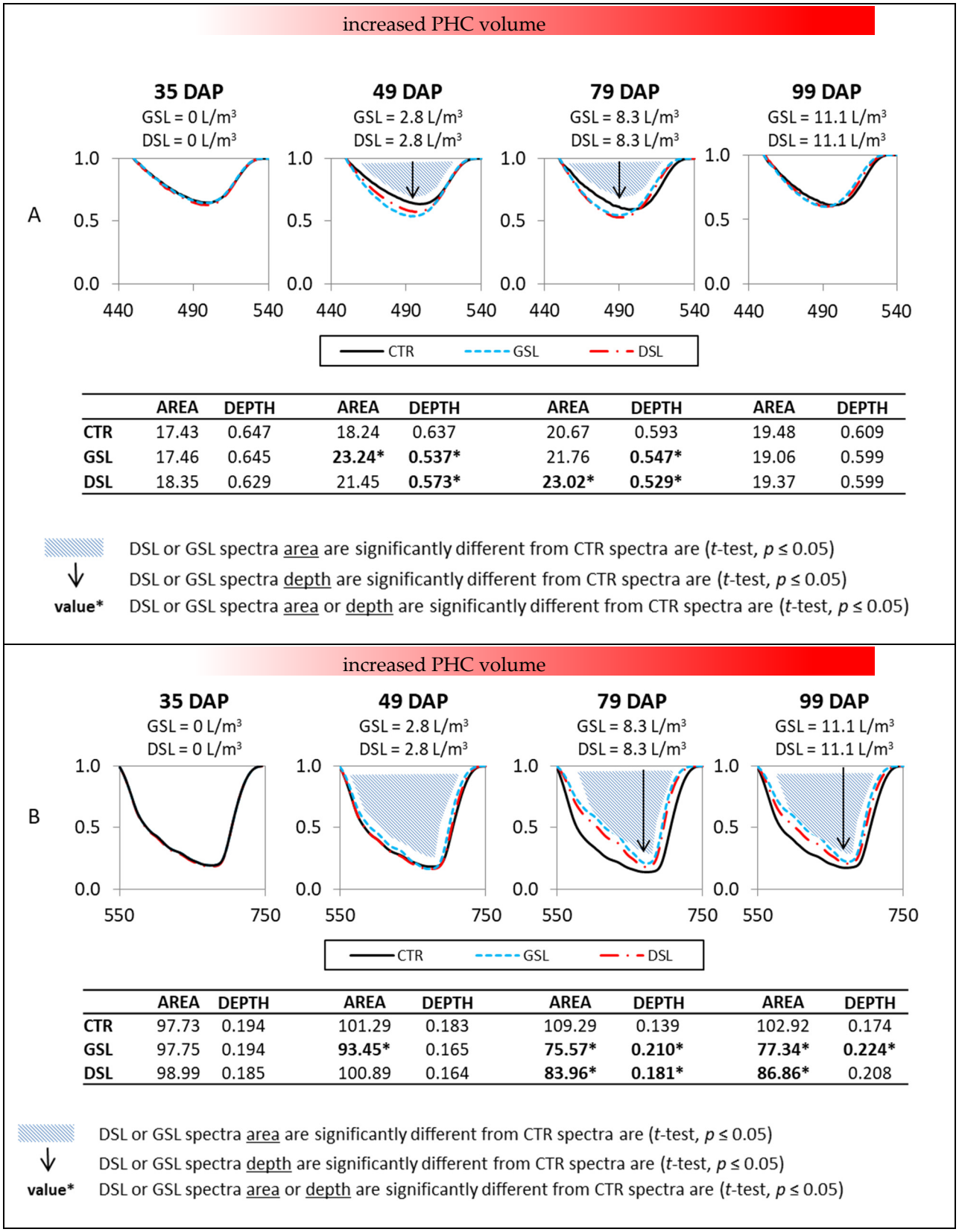

Figure 15. Leaf reflectance (SCAfter-SP) after continuum removal for the absorption features: (**A**) 450–540 nm and (**B**) 550–750 nm.

3.5. Red Edge Region

The red shift in larger wavelengths naturally occurs during plant development as chlorophyll accumulates [50]. When pigment production decreases, due to senescence or stress, REP shifts to shorter wavelengths (blue shift). Lower REP values occurred for PS contaminated with DSL under SCBefore and contaminated with DSL and GSL under SCAfter (Figures 16 and 17). Refs. [5,11,12] showed changes to plants affected by natural gas when analyzing the red edge spectrum derivative. Ref. [15] also observed REP shift to shorter wavelengths in a maize crop contaminated with different DSL volumes. Ref. [14] showed changes in the red edge (blue shift) in plants contaminated with equivalent GSL and DSL volumes (from 9.3 L/m^3 up). Ref. [50] also associated REP changes with water stress.

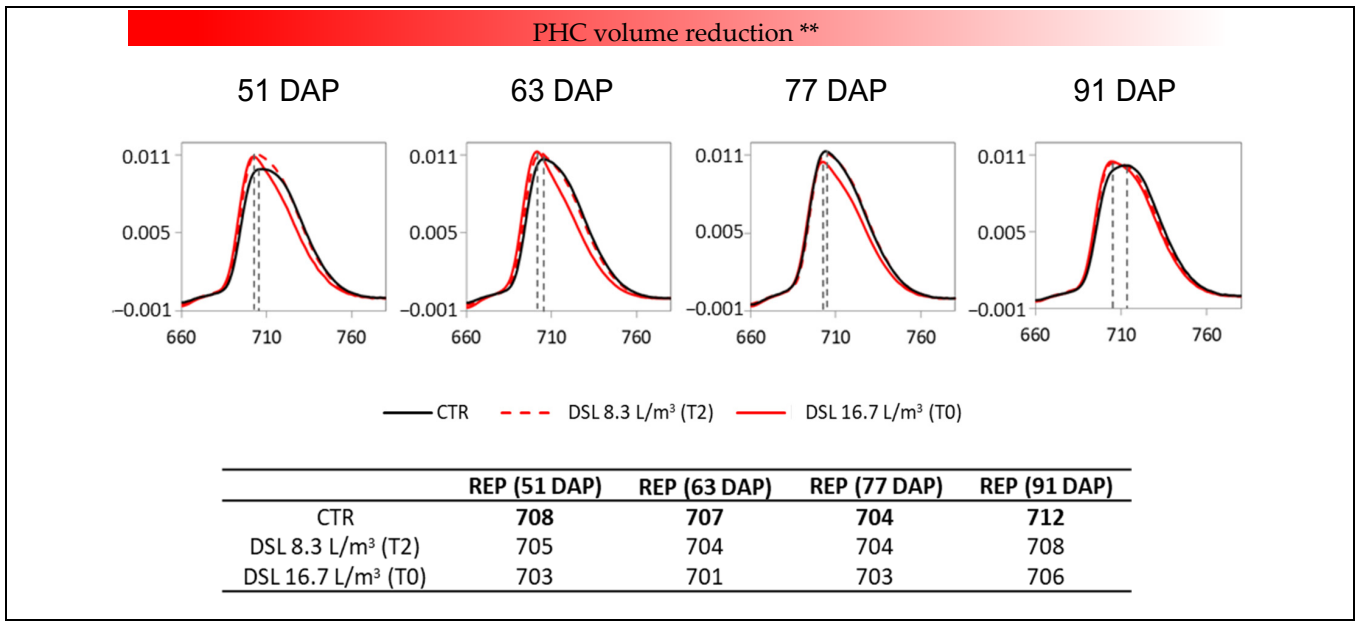

	REP (51 DAP)	REP (63 DAP)	REP (77 DAP)	REP (91 DAP)
CTR	**708**	**707**	**704**	**712**
DSL 8.3 L/m³ (T2)	705	704	704	708
DSL 16.7 L/m³ (T0)	703	701	703	706

Figure 16. First derivative of SCBefore-PS (DSL) reflectance in the red edge range, from the beginning of the development (51 DAP) to 91 DAP. ** Considering a reduction in PHC volume over time due to volatilization.

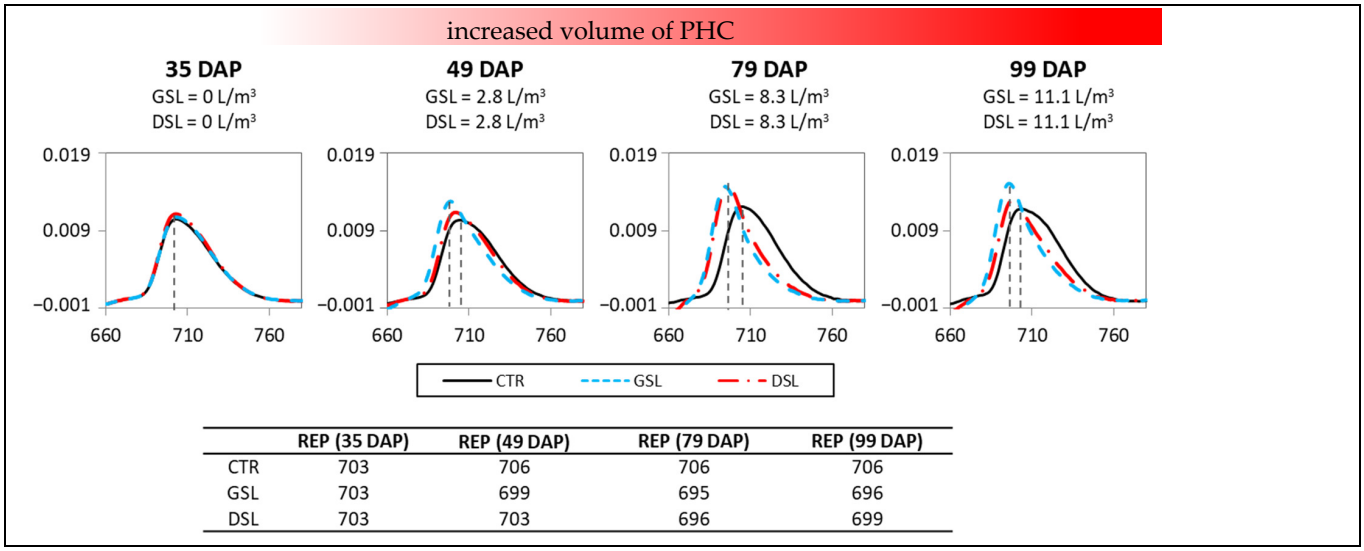

	REP (35 DAP)	REP (49 DAP)	REP (79 DAP)	REP (99 DAP)
CTR	703	706	706	706
GSL	703	699	695	696
DSL	703	703	696	699

Figure 17. First derivative of SCAfter-PS (GSL and DSL) reflectance in the red edge range, from the beginning of the development (35 DAP) to 99 DAP.

As pigment concentration in SCBefore-PS showed no decrease when compared to that of CTR, the observed blue shift might be mainly related to the plant difficulty in absorbing water in a PHC contaminated soil. Previously discussed data on water content at 90 DAP suggest that plants suffered water depletion.

Although the red edge position is more strongly associated with chlorophyll content, certain parameters (such as area and amplitude) in the first derivative graph of the red edge may be associated with other plant characteristics, such as leaf area index [50]. Considering the first derivative of BR over time, despite occupying the same position, CTR and DSL show different forms (Figure 18). The lower amplitude and width in the red edge region for the contaminated BR, especially when contaminated with DSL, occurred due to a lower spectral response in NIR (Figure 12). For SCAfter-PS, variations to both red edge position and feature form were observed (Figure 17).

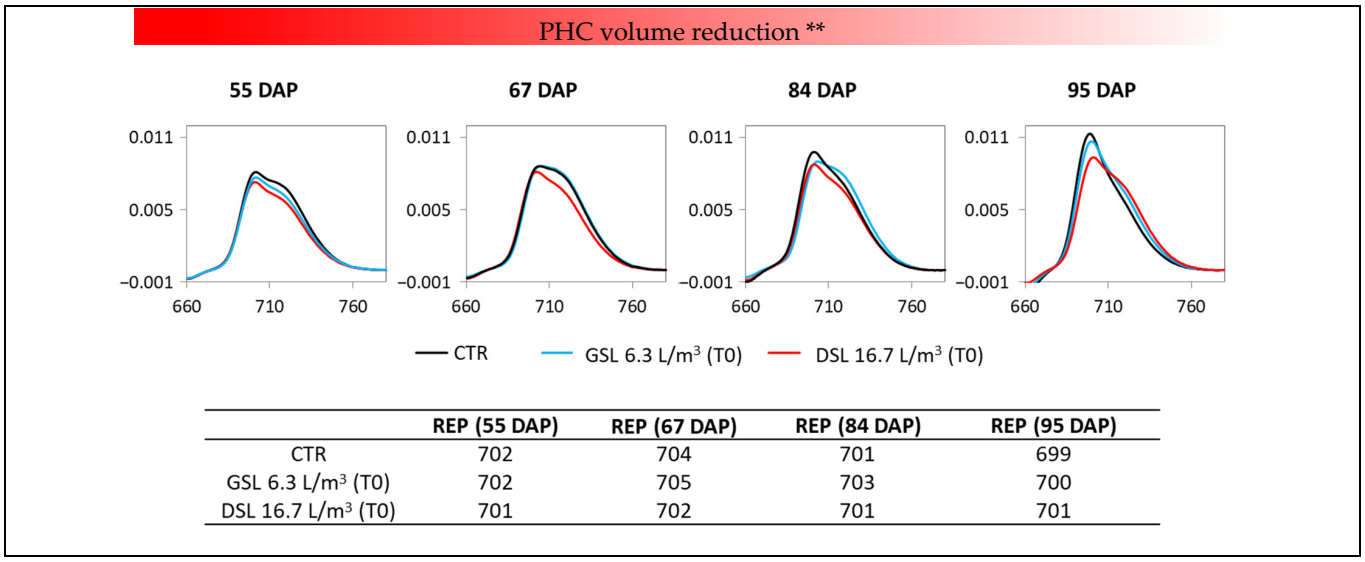

	REP (55 DAP)	REP (67 DAP)	REP (84 DAP)	REP (95 DAP)
CTR	702	704	701	699
GSL 6.3 L/m³ (T0)	702	705	703	700
DSL 16.7 L/m³ (T0)	701	702	701	701

Figure 18. First derivative of SCBefore-BR (GSL and DSL) reflectance in the red edge region, from the beginning of the development (55 DAP) to 95 DAP. ** Considering a reduction in PHC volume over time due to volatilization.

The FD725/FD702 ratio showed significant lower values (*t*-test, $p \leq 0.05$) for PS, regardless of the contamination moment (SCBefore and SCAfter-PS). For SCBefore, the index enabled identifying contamination, especially by DSL, and at a higher concentration in the soil (16.7 L/m^3) (Figure 19). All DSL concentrations and exposure times differed from those of CTR in at least one measurement, except for 8.3 L/m^3 (T2), which was considered the lowest contamination level. For SCAfter, the FD725/FD702 ratio decreased as the soil contaminant concentration increased, which was higher for GSL.

A decrease in the FD725/FD702 ratio for the spectra of plants contaminated by PHCs was verified in other studies on contamination before [47] and after plant growth [5], even in small DSL (9.3 L/m^3) and GSL (6 L/m^3) concentrations [14].

When contaminated before [47], the index performed better at distinguishing plants contaminated with diesel (8.3 L/m^3) and gasoline (6.3 L/m^3) at canopy level, but not so much at leaf level. A better performance using canopy data was expected, since leaf layers, when compared to a single leaf, augment the differences in the first derivative.

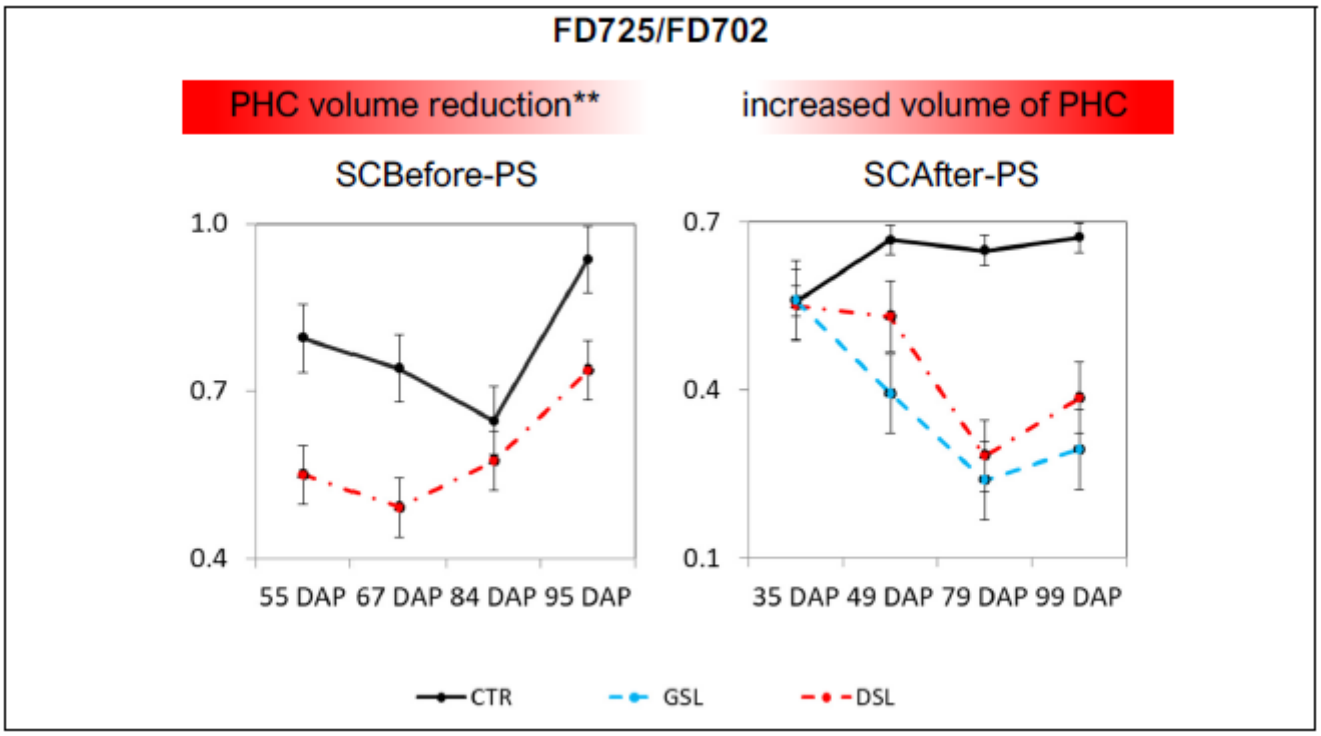

Figure 19. FD725/FD702 index for PS (SCBefore and SCAfter) at different DAPs. ** Considering a reduction in PHC volume over time due to volatilization.

4. A Possible Operational Model for a PHC Leakage Monitoring System

Given the results revealed above, it is possible to foresee a model for the potential detection of leakages in pipelines installed below the ground surface. Firstly, we strongly recommend using the planting of agricultural crops as biomarkers (as opposed to keeping the corridors along pipelines with exposed soil). Among the two species studied here, both are perennial, easy to adapt to Brazilian terrains, and have deep roots and low environmental constraints to develop. For both species, it was possible to identify spectral variations in specific bands (between 420 and 750 nm; visible and near infrared), which showed changes in the contaminated plants and could be used to identify a leak in the pipeline. By removing the continuum in the absorption features related to the pigment content (features 420–540 nm and 550–750 nm), it was shown that it is possible to enhance the effect of contaminants on plant spectra. For perennial soybean at least, the FD725/FD702 index is a promising tool. For data collection, we suggest, as an alternative to point spectroscopy, a narrow-band imaging sensor, with high spatial and temporal resolution. An alternative could be the use of VIS-RedEdge multispectral cameras (which operate in visible and red edge) on board UAVs, since the monitoring of pipelines requires a focused, linear coverage (not specifically feasible by satellites). This model could meet the objective of monitoring pipeline nets with flexibility (e.g., any time during the day, during free-cloud periods; starting the flight campaign at any section of the pipeline), using high temporal and spatial resolution. A specific drawback regarding the use of UAVs is the flight time limit imposed by the batteries. This disadvantage can be minimized by using multiple batteries, but still the UAV coverage must be halted for battery replacement. Another alternative is the use of a hyperspectral sensor on board an airplane or helicopter, but at a very high cost.

5. Conclusions

The PHCs used in this research (gasoline and diesel) affected the plants morphologically (reduction in size and fresh weight of leaves) and biochemically (changes in

chlorophyll content and vegetation water content). The biomass reduction in the experiment with contamination before planting was higher under diesel treatments, in which the applied volumes were greater than the gasoline volumes. In the experiment with contamination after planting, the same PHC volumes applied caused greater damage to the plants contaminated with gasoline.

In the experiment with contamination before planting, a failure or delay in germination caused by the PHC volatile portion affected the development of both studied species (brachiaria and perennial soybean). The biochemical analyses performed 90 days after contamination indicated that the average chlorophyll and carotenoid contents in contaminated plants were higher than or equal to those found in CTR plants. The exposure time to PHCs in the soil may have contributed to the volatile fraction reduction and decreased the contaminant toxicity. Furthermore, the plants may have increased their energy production performance to compensate for the reduction in leaf area.

The experiment with contamination after plant growth showed drastic reduction effects in pigments when the contaminations were frequent and cumulative, which hindered plant recovery.

The distinct characteristics between SCBefore (experiment with contamination before the species were planted and using different contaminant volumes applied in a single dose) and SCAfter (experiment with contamination after plant growth, with frequent contaminations that amounted to a higher accumulated PHC level) led to a better understanding of how the plants were visually, spectrally and chemically affected from germination to maturity when exposed to PHC contamination at various developmental phases.

In general, plants germinated in contaminated soil showed lower reflectance than that of healthy plants, especially in the NIR-a region influenced by the anatomic structure of the leaf. In SCBefore, the contaminants affected the plant vegetative development, while in SCAfter, in which contaminants were applied after the plant growth, PHCs caused a reflectance increase when compared to that of CTR. A pigment content reduction in stressed plants decreased absorption in the VIS region, increasing the spectral response.

Red edge absorption features and parameters (red edge position and FD725/FD702 ratio) demonstrated the detected spectral, morphological, and biochemical changes. In the experiment with contamination before planting, there were changes to pigment absorption features, water absorption features and REP for the contaminated plants. In the experiment with continuous contamination after plant growth, we detected typical changes in plants biochemically affected, with a reduction in the pigment absorption feature, blue shift in red edge position and a reduction in the FD725/FD702 ratio.

More comprehensive studies may show the complexity of indirectly identifying PHC soil contamination by means of anomalies in vegetation spectra. Reducing the plant germination index and inhibiting plants' initial development not only affect leaf area index but also render contamination more evident. Since several PHC transportation pipelines pass through commercial crop areas, their canopy analyses may detect lower spectral responses in vegetation, or even in the soil, which might indicate contaminant leakage.

This novel approach for detecting contamination effects, in all plant developmental phases, makes it an important reference for tests and applications of this indirect detection method, which uses hyperspectral data obtained from sensors onboard UAVs, planes, and satellites. Therefore, there is a need to evaluate an economically viable model for monitoring pipeline networks from an operational point of view, since the model must take into account a high revisiting frequency for data collection, high spatial resolution, as well as rising demand for data processing to detect spectral changes.

Author Contributions: Conceptualization, C.R.S.F. and W.J.O.; Funding acquisition, W.J.O.; Investigation, S.G., L.A.M. and G.C.M.Q.; Methodology, S.G., C.R.S.F., I.D.S., L.A.M. and G.C.M.Q.; Project administration, S.G. and M.N.A.; Resources, M.N.A. and W.J.O.; Supervision, C.R.S.F. and I.D.S.; Validation, S.G.; Visualization, S.G. and W.J.O.; Writing—original draft, S.G.; Writing—review & editing, S.G., C.R.S.F. and G.C.M.Q. All authors have read and agreed to the published version of the manuscript.

Funding: This research was funded by National Council for Scientific and Technological Development (CNPq), grant number 309712/2017-3; Centro de Pesquisas e Desenvolvimento (CENPES) of PETROBRAS, grant number Project Biomarkers I.

Acknowledgments: S. Gürtler is grateful to CNPq for the scholarship. The authors want to express their thanks to the management and researchers of the Programa Tecnológico de Transporte (PROTRAN) in the Centro de Pesquisas e Desenvolvimento (CENPES) of Petrobras, especially Pedro Altoe Ferreira, Lis Maria Leoni Rabaco and Renato Seixas da Rocha.

Conflicts of Interest: The authors declare no conflict of interest.

References

1. ANP—Agência Nacional do Petróleo, Gás Natural e Biocombustíveis. *Anuário Estatístico Brasileiro do Petróleo, Gás Natural e Biocombustíveis*; ANP: Brasília, Brasil, 2014. Available online: http://www.anp.gov.br/?pg=73222&m=&T1=&T2=&t3=&t4=&ar=&ps=&cachebust=1425483461560 (accessed on 15 March 2015).
2. Lassalle, G.; Fabre, S.; Credoz, A.; Dubucq, D.; Elger, A. Monitoring oil contamination in vegetated areas with optical remote sensing: A comprehensive review. *J. Hazard. Mater.* **2020**, *393*, 1224272. [CrossRef] [PubMed]
3. Meribout, M.; Khezzar, L.; Azzi, A.; Ghendour, N. Leak detection systems in oil and gas fields: Present trends and future prospects. *Flow Meas. Instrum.* **2020**, *75*, 101772. [CrossRef]
4. Kechavarzi, C.; Pettersson, K.; Leeds-Harrison, P.; Ritchie, L.; Ledin, S. Root establishment of *Perennial ryegrass* (L. perenne) in diesel contaminated subsurface soil layers. *Environ. Pollut.* **2007**, *145*, 68–74. [CrossRef] [PubMed]
5. Smith, K.L.; Steven, M.D.; Colls, J.J. Use of hyperspectral derivative ratios in the red-edge region to identify plant stress responses to gas leaks. *Remote Sens. Environ.* **2004**, *92*, 207–217. [CrossRef]
6. Wyszkowski, M.; Wyszkowska, J. Effect of enzymatic activity of diesel oil contaminated soil on the chemical composition of oat (*Avena sativa* L.) and maize (*Zea mays* L.). *Plant Soil Environ.* **2005**, *51*, 360–367. [CrossRef]
7. Ourcival, J.; Joffre, R.; Rambal, S. Exploring the relationships between reflectance and anatomical and biochemical properties in Quercus ilex leaves. *New Phytol.* **1999**, *143*, 351–364. [CrossRef]
8. Jensen, J.R. *Remote Sensing of the Environment: An Earth Resource Perspective*; Prentice Hall Series in Geographic Information Science; Prentice-Hall: Upper Saddle River, NJ, USA, 2000; 544p, ISBN 0134897331.
9. van der Meijde, M.; van der Werff, H.M.A.; Kooistra, J.F. Detection of Spectral Features of Anomalous Vegetation from Reflectance Spectroscopy Related to Pipeline Leakages. In Proceedings of the 2004 AGU Fall Meeting, San Francisco, CA, USA, 13–17 December 2005. Available online: http://www.itc.nl/library/Papers_2004/abstract/vandermeijde_detection.pdf (accessed on 27 November 2011).
10. Noomen, M.F.; Skidmore, A.K.; van der Meer, F.D.; Prins, H.H.T. Continuum removed band depth analysis for detecting the effects of natural gas, methane and ethane on maize reflectance. *Remote Sens. Environ.* **2006**, *105*, 262–270. [CrossRef]
11. Noomen, M.F.; Smith, K.L.; Colls, J.J.; Steven, M.D.; Skidmore, A.K.; van der Meer, F.D. Hyperspectral indices for detecting changes in canopy reflectance as a result of underground natural gas leakage. *Int. J. Remote Sens.* **2008**, *29*, 5987–6008. [CrossRef]
12. Noomen, M.F.; van der Werff, H.M.A.; van der Meer, F.D. Spectral and spatial indicators of botanical changes caused by long-term hydrocarbon seepage. *Ecol. Inform.* **2012**, *8*, 55–64. [CrossRef]
13. Sanches, I.D.; Souza Filho, C.R.; Magalhães, L.A.; Quitério, G.C.M.; Alves, M.N.; Oliveira, W.J. Assessing the impact of hydrocarbon leakages on vegetation using reflectance spectroscopy. *ISPRS J. Photogramm. Remote Sens.* **2013**, *78*, 85–101. [CrossRef]
14. Sanches, I.D.; Souza Filho, C.R.; Magalhães, L.A.; Quitério, G.C.M.; Alves, M.N.; Oliveira, W.J. Unravelling remote sensing signatures of plants contaminated with gasoline and diesel: An approach using the red edge spectral feature. *Environ. Pollut.* **2013**, *174*, 16–27. [CrossRef] [PubMed]
15. Emengini, E.J.; Blackburn, G.A.; Theobald, J.C. Early detection of oil-induced stress in crops using spectral and thermal responses. *J. Appl. Remote Sens.* **2013**, *7*, 15. [CrossRef]
16. Emengini, E.J.; Blackburn, G.A.; Theobald, J.C. Discrimination of plant stress caused by oil pollution and waterlogging using hyperspectral and thermal remote sensing. *J. Appl. Remote Sens.* **2013**, *7*, 17. [CrossRef]
17. Noomen, M.; Hakkarainen, A.; van der Meijde, M.; van der Werff, H. Evaluating the feasibility of multitemporal hyperspectral remote sensing for monitoring bioremediation. *Int. J. Appl. Earth Obs. Geoinf.* **2015**, *34*, 217–225. [CrossRef]
18. Arellano, P.; Tansey, K.; Balzter, H.; Boyd, D.S. Detecting the effects of hydrocarbon pollution in the Amazon forest using hyperspectral satellite images. *Environ. Pollut.* **2015**, *205*, 225–239. [CrossRef] [PubMed]
19. Adamu, B.; Tansey, K.; Ogutu, B. Remote sensing for detection and monitoring of vegetation affected by oil spills. *Int. J. Remote Sens.* **2018**, *39*, 3628–3645. [CrossRef]
20. Gholizadeh, A.; Kopačková, V. Detecting vegetation stress as a soil contamination proxy—A review of optical proximal and remote sensing techniques. *Int. J. Environ. Sci. Technol.* **2019**, *16*, 2511–2524. [CrossRef]
21. Curran, P.J. Remote sensing of foliar chemistry. *Remote Sens. Environ.* **1989**, *30*, 271–278. [CrossRef]
22. Curran, P.J.; Dungan, J.L.; Macler, B.A.; Plummer, S.E.; Peterson, D.L. Reflectance spectroscopy of fresh whole leaves for the estimation of chemical concentration. *Remote Sens. Environ.* **1992**, *39*, 153–166. [CrossRef]

23. Kokaly, R.F.; Clark, R.N. Spectroscopic determination of leaf biochemistry using band-depth analysis of absorption features and stepwise multiple linear regression. *Remote Sens. Environ.* **1999**, *67*, 267–287. [CrossRef]
24. Kumar, L.; Schmidt, K.; Dury, S.; Skidmore, A. Imaging spectrometry and vegetation science. In *Imaging Spectrometry: Basic Principles and Prospective Applications*; van der Meer, F.D., Jong, S.M., Eds.; Springer: Dordrecht, The Netherlands, 2001; Volume 4, pp. 111–155.
25. Serrano, A.; Tejada, M.; Gallego, M.; Gonzalez, J.L. Evaluation of soil biological activity after a diesel fuel spill. *Sci. Total Environ.* **2009**, *407*, 4056–4061. [CrossRef] [PubMed]
26. Adam, G.; Duncan, H. Influence of diesel fuel on seed germination. *Environ. Pollut.* **2002**, *120*, 363–370. [CrossRef]
27. ASD—Analytical Spectral Devices. *ASD Accessories User Manual*; ASD Document 600544; ASD Inc.: Boulder, CO, USA, 2007; 120p.
28. ASD—Analytical Spectral Devices. *FieldSpec 4 User Manual*; ASD Document 600979; ASD Inc.: Boulder, CO, USA, 2012; 98p.
29. Kokaly, R.F. *PRISM: Processing Routines in IDL for Spectroscopic Measurements*; Installation Manual and User's Guide, Version 1.0; U.S. Geological Survey Open-File Report 2011–1155; USGS: Reston, VA, USA, 2011; 432p. Available online: http://pubs.usgs.gov/of/2011/1155/ (accessed on 1 January 2014).
30. Kokaly, R.F. Investigating a physical basis for spectroscopic estimates of leaf nitrogen concentration. *Remote Sens. Environ.* **2001**, *75*, 153–161. [CrossRef]
31. Yang, H.; van der Meer, F.D.; Zhang, J. Aerospace detection of hydrocarbon-induced alteration. In *Geochemical Remote Sensing of the Subsurface*; Handbook of Exploration Geochemistry; Hale, M., Govett, G.J.S., Eds.; Elsevier: Amsterdam, The Netherlands, 2000; Volume 7, pp. 233–245.
32. Horler, D.N.H.; Dockray, M.; Barber, J. The red edge of plant leaf reflectance. *Int. J. Remote Sens.* **1983**, *4*, 273–288. [CrossRef]
33. Dawson, T.P.; Curran, P.J. A new technique for interpolating the reflectance red edge position. *Int. J. Remote Sens.* **1998**, *19*, 2133–2139. [CrossRef]
34. van der Meijde, M.; van der Werff, H.M.A.; Jansma, P.F.; van der Meer, F.D.; Groothuis, G.J. A spectral-geophysical approach for detecting pipeline leakage. *Int. J. Appl. Earth Obs. Geoinf.* **2009**, *11*, 77–82. [CrossRef]
35. CAMO. *The Unscrambler Appendices: Method References*; Aspen Tech: Bedford, MA, USA, 2014; 45p. Available online: http://www.camo.com/helpdocs/The_Unscrambler_Method_References.pdf (accessed on 27 November 2014).
36. Ceccato, P.; Flasse, S.; Tarantola, S.; Jacquemoud, S.; Grégoire, J.M. Detecting Vegetation Leaf Water Content Using Reflectance in the Optical Domain. *Remote Sens. Environ.* **2001**, *77*, 22–33. [CrossRef]
37. Xia, H.; Ma, X. Phytoremediation of ethion by water hyacinth (*Eichhornia crassipes*) from water. *Bioresour. Technol.* **2006**, *97*, 1050–1054. [CrossRef]
38. Al-Baldawi, I.A.; Abdullah, S.R.S.; Anuar, N.; Suja, F.; Mushrifah, I. Phytodegradation of total petroleum hydrocarbon (TPH) in diesel-contaminated water using *Scirpus grossus*. *Ecol. Eng.* **2015**, *74*, 463–473. [CrossRef]
39. Sharonova, N.; Breus, I. Tolerance of cultivated and wild plants of different taxonomy to soil contamination by kerosene. *Sci. Total Environ.* **2012**, *424*, 121–129. [CrossRef]
40. Balseiro-Romero, M.; Monterroso, C. Phytotoxicity of fuel to crop plants: Influence of soil properties, fuel type, and plant tolerance. *Toxicol. Environ. Chem.* **2015**, *2248*, 1–12. [CrossRef]
41. Siddiqui, S.; Adams, W.A. The Fate of Diesel Hydrocarbons in Soils and Their Effect on the Germination of Perennial Ryegrass. *Environ. Toxicol.* **2002**, *17*, 49–62. [CrossRef]
42. Adam, G.; Duncan, H. The Effect of Diesel Fuel on Common Vetch (*Vicia sativa* L.) Plants. *Environ. Geochem. Health* **2003**, *25*, 123–130. [CrossRef] [PubMed]
43. Liew, O.W.; Chong, P.C.J.; Li, B.; Asundi, A.K. Signature optical cues: Emerging technologies for monitoring plant health. *Sensors* **2008**, *8*, 3205–3239. [CrossRef] [PubMed]
44. Barrutia, O.; Garbisu, C.; Epelde, L.; Sampedro, M.C.; Goicolea, M.A.; Becerril, J.M. Plant tolerance to diesel minimizes its impact on soil microbial characteristics during rhizoremediation of diesel-contaminated soils. *Sci. Total Environ.* **2011**, *409*, 4087–4093. [CrossRef] [PubMed]
45. Smith, K.L.; Steven, M.D.; Colls, J.J. Plant spectral responses to gas leaks and other stresses. *Int. J. Remote Sens.* **2005**, *26*, 4067–4081. [CrossRef]
46. Wang, J.; Liu, X.; Zhang, X.; Liang, X.; Zhang, W. Growth response and phytoremediation ability of Reed for diesel contaminant. *Procedia Environ. Sci.* **2011**, *8*, 68–74. [CrossRef]
47. Gürtler, S.; Souza Filho, C.R.; Sanches, I.D.; Alves, M.N.; Oliveira, W.J. Determination of changes in leaf and canopy spectra of plants grown in soils contaminated with petroleum hydrocarbons. *ISPRS J. Photogramm. Remote Sens.* **2018**, *146*, 272–288. [CrossRef]
48. Lassalle, G.; Credoz, A.; Hédacq, R.; Fabre, S.; Dubucq, D.; Elger, A. Assessing Soil Contamination Due to Oil and Gas Production Using Vegetation Hyperspectral Reflectance. *Environ. Sci. Technol.* **2018**, *52*, 1756–1764. [CrossRef]
49. Slaton, M.; Hunt, E.; Smith, W. Estimating near-infrared leaf reflectance from leaf structural characteristics. *Am. J. Bot.* **2001**, *88*, 278–284. [CrossRef]
50. Filella, I.; Penuelas, J. The red edge position and shape as indicators of plant chlorophyll content, biomass and hydric status. *Int. J. Remote Sens.* **1994**, *15*, 1459–1470. [CrossRef]